

**AN EXPERIMENTAL STUDY OF FACTORS AFFECTING HYPERGOLIC  
IGNITION OF AMMONIA BORANE**

by

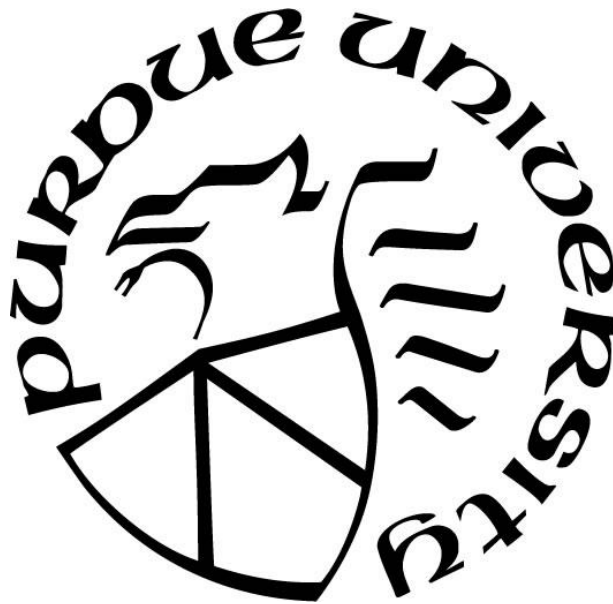
**Kathryn A. Clements**

**A Thesis**

*Submitted to the Faculty of Purdue University*

*In Partial Fulfillment of the Requirements for the degree of*

**Master of Science in Mechanical Engineering**



School of Mechanical Engineering

West Lafayette, Indiana

May 2020

**THE PURDUE UNIVERSITY GRADUATE SCHOOL  
STATEMENT OF COMMITTEE APPROVAL**

**Dr. Steven Son, Chair**

School of Mechanical Engineering

**Dr. Timothée Pourpoint**

School of Aeronautics and Astronautics

**Dr. Terrence Meyer**

School of Mechanical Engineering

**Approved by:**

Dr. Steven Son

*Dedicated to Grandma Isabelle*

## ACKNOWLEDGMENTS

I would like to gratefully acknowledge the National Science Foundation Graduate Research Fellowship Program (grant number DGE-1333468) and Purdue's Laura Winkelman Davidson Fellowship for their educational financial support, as well as the Army Research Office (grant number W911NF-15-1-0201) for their financial support of this project. Additionally, some experimental equipment and supplies for this project were purchased through a NASA Space Technology Research Fellowship (grant number 80NSSC17K0177).

I would like to thank my advisor, Prof. Steve Son, for the opportunity to pursue propellant research, as well as Prof. Timothée Pourpoint and Prof. Terry Meyer for serving on my thesis committee. I would also like to thank Prof. Ramachandran for his contributions to my paper as a co-author.

I sincerely thank all my friends, labmates, and colleagues at Zucrow Laboratories and affiliated labs for lending their insights and expertise in addition to making this experience a whole lot more fun. I would especially like to thank Michael Baier for his assistance in running the ignition delay experiments and his input on this project and my paper, Spencer Fehlberg for his assistance with WFNA transfer and other aspects of my projects, and Tim Manship for his valuable input on all of my projects. I would also like to thank Scott Meyer and Jason Gabl for answering my incessant questions about rocket plumbing, Taylor Groom for his help with taking AB purity measurements, Henry Hamann for performing boron NMR, Matt Gettings for his help with FTIR spectroscopy, Blair Francis for his help measuring contact angles, Alex Casey for his help with statistical analysis, Zane Roberts for his video editing guidance, Prof. Davin Piercey for his insights on phosphorous pentoxide usage as well as my other project, and Robert McGuire for his help with fabricating part of the test apparatus. In addition, I thankfully acknowledge Jen Ulutas, Tania Bell, Michelle Kidd, Michelle Moody, and Sheri Tague for their administrative and purchasing assistance.

I would like to thank the Catholic Adults Living in Lafayette in their 20s and 30s group for their friendship and the St. Thomas Aquinas parish for the many opportunities to grow in my faith during my time at Purdue.

I am deeply thankful for and my friends and family. I would like to thank my grandparents for our conversations which always fill me with love, joy, and purpose. I would like to thank my

dear friends, especially Val, Nick, Anna, Alexis, and Claire, for their visits, chats, encouragement, and many laughs, as well as my boyfriend Neil for his companionship. Finally, I would like to thank my parents and brother for their unwavering love and support of me and my dreams.

# TABLE OF CONTENTS

LIST OF TABLES .....	8
LIST OF FIGURES .....	9
LIST OF ABBREVIATIONS AND SYMBOLS .....	10
ABSTRACT.....	11
1. INTRODUCTION .....	12
2. LITERATURE REVIEW .....	14
2.1 Introduction.....	14
2.2 Ignition Processes .....	15
2.2.1 Preignition Processes.....	15
2.2.2 Surface Reactions .....	16
2.3 Ignition of Amine-Boranes .....	17
2.4 Factors Affecting Ignition Delay .....	19
2.4.1 Compactness .....	19
2.4.2 Fuel Particle Diameter .....	20
2.4.3 Temperature.....	20
2.4.4 Pressure.....	21
2.4.5 Amount or Ratio .....	21
2.4.6 Oxidizer Concentration.....	23
2.4.7 Binder .....	23
2.4.8 Additives.....	24
2.5 Ignition in Motor Environment.....	25
2.6 Conclusion .....	26
3. METHODS .....	27
3.1 Fuel Powder .....	27
3.2 Fuel Pellets.....	28
3.3 Ignition Delay Tests.....	28
3.4 Wetting Contact Angle Tests .....	31
4. RESULTS .....	33

4.1	Droplet Impact Velocity .....	33
4.2	Solids Loading .....	34
4.2.1	AB Pellet Results.....	34
4.2.2	Comparison to EDBB .....	37
4.2.3	Role of Binder.....	39
4.2.4	Reignition .....	43
4.3	Storage Conditions.....	43
5.	DISCUSSION AND CONCLUSION .....	46
	APPENDIX A. WFNA TRANSFER PROCEDURE.....	48
	APPENDIX B. DROPLET TEST PROCEDURE.....	54
	REFERENCES .....	60
	PUBLICATIONS.....	63

## LIST OF TABLES

Table 4.1. Numerical results of varying droplet impact velocity. ....	34
Table 4.2. Numerical results of varying solids loading. ....	35
Table 4.3. Numerical results of varying solids loading of sanded but unbrushed pellets.....	37
Table 4.4. Comparison of AB initial ignition delays versus those of EDBB. ....	38
Table 4.5. Contact angles between WFNA and various binders. ....	41
Table 4.6. Numerical results of varying storage humidity.....	45

## LIST OF FIGURES

Figure 2.1. Ignition of EDBB powder with WFNA [2].	18
Figure 2.2. Violent reaction of EDBB pellet with WFNA [2].	19
Figure 2.3. Specific impulse of hypergolic fuels with IRFNA IIIA [4].	22
Figure 3.1. Equipment used for fuel pellet preparation: oven (left), dry box (center), and Carver press (right).	28
Figure 3.2. Droplet test configuration.	29
Figure 3.3. Image sequence of ignition delay test of 80% AB pellet with WFNA.	30
Figure 3.4. Image sequence of test with separate initial and main ignitions.	30
Figure 3.5. Example of normal distribution to which ANOVA was applied.	31
Figure 3.6. Sample image used for initial contact angle measurement of WFNA on RTV.	32
Figure 4.1. Ignition delay of 80% AB pellets as a function of droplet impact velocity based on initial ignition (left) and main ignition (right).	34
Figure 4.2. Ignition delay of AB pellets as a function of solids loading based on initial ignition (left) and main ignition (right).	35
Figure 4.3. Ignition delay of AB pellets from which residual powder from sanding was not removed based on initial ignition (left) and main ignition (right).	37
Figure 4.4. Graphical comparison of AB initial ignition delays versus those of EDBB.	39
Figure 4.5. Untouched epoxy pellet (left) compared to epoxy pellet after being contacted with WFNA and rinsed with DI water (right).	39
Figure 4.6. Comparison of WFNA splashing immediately following droplet impact with plain epoxy pellet (top) and neat AB pellet (bottom).	40
Figure 4.7. EDBB cut pellet ignition delays versus initial contact angles for the binders used.	41
Figure 4.8. EDBB sanded pellet ignition delays versus initial contact angles for the binders used.	42
Figure 4.9. EDBB pellet ignition delays versus steady-state contact angles for the binders used.	42
Figure 4.10. Ignition delay of 80% solids loading AB pellets as a function of pellet storage for initial ignition (left) and main ignition (right).	44

## LIST OF ABBREVIATIONS AND SYMBOLS

AB	=	ammonia borane
ANOVA	=	analysis of variance
C*	=	characteristic velocity
DI	=	deionized
EDBB	=	ethylenediamine-bisborane
FTIR	=	Fourier-transform infrared
HCl	=	hydrochloric acid
HTPB	=	hydroxyl-terminated polybutadiene
ID	=	ignition delay
IRFNA	=	inhibited red fuming nitric acid
$I_{sp}$	=	specific impulse
MON	=	mixed oxides of nitrogen
NMR	=	nuclear magnetic resonance
NTO	=	dinitrogen tetroxide ( $N_2O_4$ )
O/F	=	oxidizer to fuel ratio
PTFE	=	polytetrafluoroethylene (Teflon)
RFNA	=	red fuming nitric acid
RH	=	relative humidity
TMD	=	theoretical maximum density
$\tau$	=	ignition delay
WFNA	=	white fuming nitric acid ( $HNO_3$ )

## ABSTRACT

Hypergolic hybrid motors are advantageous for rocket propulsion due to their simplicity, reliability, low weight, and safety. Many hypergolic hybrid fuels with promising theoretical performance are not practical due to their sensitivity to temperature or moisture. Ammonia borane (AB) has been proposed and studied as a potential hypergolic hybrid fuel that provides both excellent performance and storability. This study investigates the effect of droplet impact velocity, pellet composition, and storage humidity on ignition delay of AB with white fuming nitric acid as the oxidizer. Most ignition delays measured were under 50 ms with many under 10 ms and some even under 2 ms, which is extremely short for hybrid systems. Higher droplet velocities led to slightly shorter ignition delays, and exposing samples to humidity slightly increased ignition delay. An AB pellet composition of at least 20% epoxy binder was found to minimize ignition delay. The epoxy facilitates ignition by absorbing or adhering the oxidizer and slowing the reaction with the fuel, preventing oxidizer expulsion and holding it close to the fuel. These results emphasize the importance of binder properties in hypergolic hybrids. Pellets varying in composition and storage method were extinguished and reignited with the oxidizer to demonstrate reignition capability.

# 1. INTRODUCTION

While there are many methods of ignition in existence, hypergolic ignition is uniquely advantageous for rocket applications due to its simplicity, reliability, and reignition capability [1]. Other ignition systems add complexity and can often only be used once. Most hypergolic propellant combinations use toxic fuels and oxidizers that are both liquids. Using a solid fuel instead of a liquid fuel, however, saves weight and complexity, because it eliminates one of the fluid systems. Hypergolic hybrid configurations offer the additional advantage of safety over their liquid counterparts. Liquid systems are susceptible to hard starts when too much propellant is released into the chamber before igniting causing an overpressurization and subsequent explosion of the fuel-oxidizer mixture. Hybrids, on the other hand, mitigate this risk, because the solid state of the fuel prevents it from mixing intimately with the oxidizer in large quantities. Similarly, hybrids are considered safer than solid propellants, because the fuel and oxidizer are separate in a hybrid system as opposed to being stored already mixed as in a solid propellant. Hypergolic hybrid motors also have advantages over non-hypergolic hybrid motors which typically have lower regression rates and require relatively large amounts of energy to start [2].

Ignition delay (ID) is the time from initial fuel-oxidizer contact to ignition, and it is one of the most important criteria for characterizing hypergolic propellant combinations. While this is more of a concern in liquid systems due to their risk of hard start, it is still an important metric for hybrid systems if they are to provide accurate attitude control [1] or rapid ignition for any other application requiring it. Other important criteria that are often prohibitive of otherwise promising fuels are long-term storability and insensitivity to moisture. Many metal hydrides and amines fall into this category due to their lack of stability in humid conditions.

Amine-boranes are promising answers to this problem due to their long-term storability and low toxicity [3] in addition to their IDs being some of the shortest ever recorded for hypergolic hybrids [4]. They also boast theoretical performance comparable to or higher than several liquid hypergolic fuels [1, 4, 5]. Some amine-boranes, such as ethylenediamine-bisborane (EDBB) and ammonia borane (AB), have two peaks of theoretical specific impulse ( $I_{sp}$ ) with respect to oxidizer-to-fuel ratio (O/F) as opposed to the typical single peak [4, 6]. This is advantageous, because it allows a motor to maintain high performance over a wider range of operating conditions including ignition, throttling, and shutdown transients.

AB ( $\text{NH}_3\text{BH}_3$ ) is a promising amine-borane, because it has the shortest ID of the amine-boranes tested by Pfeil [1], Pfeil and Dailey [3], and Ramachandran et al. [5] and the highest theoretical  $I_{sp}$  of all the hypergolic fuels examined by Pfeil et al. [4]. Baier et al. measured AB IDs as short as 0.6 ms [6], while Ramachandran et al. consistently measured 2 ms [5], and Pfeil and Dailey measured as short as 1 ms [3]. The high theoretical  $I_{sp}$  and characteristic velocity ( $C^*$ ) are due to AB's high hydrogen content of 19.6% by mass which results in significant  $\text{H}_2$  release upon AB decomposition and low molecular weight combustion products [7]. Weismiller et al. experimentally confirmed these benefits to  $I_{sp}$  and  $C^*$  by including AB as an additive in a non-hypergolic hybrid motor.

The purpose of this work is to characterize AB for use in hypergolic hybrid propulsion systems and to specifically examine the effects that varying certain experimental parameters has on ID and the reignition capability of extinguished fuel pellets. Factors investigated include fuel pellet composition, oxidizer droplet impact velocity, and storage humidity. Effects discovered have potential implications on how solid fuel grains for hypergolic hybrid motors should be designed, fabricated, and stored.

## 2. LITERATURE REVIEW

### 2.1 Introduction

Hypergolic ignition is a process in which fuel and oxidizer ignite almost instantaneously upon coming into contact with each other without any additional input [1]. While other methods of ignition exist, hypergolic ignition is advantageous for rocket applications for multiple reasons. Separate ignition systems require additional hardware, adding weight and complexity, and can typically only be used once. The utilization of hypergolic ignition allows for restarts while adding simplicity and reliability.

Most hypergolic propellant combinations are entirely liquid. However, there has been a significant amount of study into hypergolic hybrid propellants which involve a solid fuel and a liquid oxidizer. Using solid fuel instead of liquid fuel eliminates one of the fluid systems, thus saving weight and decreasing complexity. Additionally, hybrid hypergols are not susceptible to hard starts like liquid hypergols, because the solidity of the fuel makes large-scale intimate mixing of the fuel and oxidizer extremely unlikely [1]. Hypergolic hybrid motors are also advantageous over more traditional, non-hypergolic hybrid motors. Their hypergolicity leads to higher regression rates, and they do not require the large amounts of energy to start that non-hypergolic hybrid motors typically do [2].

Two criteria for a good hypergolic propellant combination are ignition delay (ID) and performance. ID is the time between initial fuel-oxidizer contact and ignition, and it will be the focal point of this review. Performance is usually characterized by specific impulse ( $I_{sp}$ ) and/or density specific impulse ( $\rho I_{sp}$ ). However, other criteria include long-term storability (especially sensitivity to moisture), stability, temperature sensitivity, reactivity, and toxicity [1]. These criteria often prove to be preventative of use. For example, many amines and metal hydrides have promising performance characteristics, but they are not stable in humid conditions, thus making them impractical to manufacture and store for long periods of time [2]. Additionally, metal hydrides are commonly toxic and pyrophoric. Until recently, there were no known hybrid hypergol combinations that satisfied these requirements while also having performance superior to that of liquid hypergols. Therefore, liquid hypergol systems continue to dominate.

ID is a critical parameter in liquid hypergolic engines, because too long of an ignition delay can lead to a hard start. Although hard starts are not a threat to hypergolic hybrid systems, ignition delay is still important for applications such as dynamic attitude control [1]. The shorter the ignition delay, the more accurate the attitude control possible.

In order to find or create a hypergolic hybrid combination that would satisfy all the criteria provided, studies regarding the process of hypergolic ignition and the factors affecting ignition delay were performed and will serve as the basis of this review.

Hypergolic hybrid systems are currently being studied for potential use on the Mars Ascent Vehicle (MAV) due to the low temperature sensitivity required as well as for their simple and storable nature [8]. Another potential application for hypergolic hybrid systems is in-space propulsion, because of the high  $I_{sp}$  and storability required [7].

## **2.2 Ignition Processes**

### **2.2.1 Preignition Processes**

Jain and Rajendran performed extensive work into the study of preignition reactions in hypergolic combustion of hybrid propellants [9]. The main reactions responsible for hypergolic ignition for simple organic (C, H, N) fuels are neutralization, oxidation, and nitration often occurring simultaneously. These reactions may produce unstable intermediates which decompose exothermically [10]. They pointed out that the lack of understanding of these reactions makes prediction of hypergolicity difficult [9]. More knowledge of these reactions could theoretically allow ignition delays to be decreased by putting the appropriate functional groups in fuel molecules to facilitate these reactions.

They used various bithiocarbonhydrazones and thiosemicarbazones as their fuels and white fuming nitric acid (WFNA) and red fuming nitric acid (RFNA) as their oxidizers. They had performed previous work with monothiocarbonhydrazones as their fuel, and these data points were used for comparison. They diluted their fuels with inert glass powder to dissipate the heat generated without affecting the fuels' physiochemical properties. Experiments were conducted in a sealed glass container flushed with helium. WFNA was added in such a way that there was reaction but no ignition. By quenching the reactions that would normally lead to ignition,

intermediate species were isolated in the form of residue and gas phase products and could then be analyzed. IDs were used for analysis in cases when they let the reactions proceed to ignition.

Although they were unable to isolate a salt to prove the neutralization reaction, the fact that ignition was more reliable with shorter delay using WFNA than using RFNA in every case except one suggested the prominence of neutralization. It is worth noting that Bernard et al. noticed crystals with circular nuclei on the surface of their fuel particles indicating the presence of a salt [11]. This led them to form a hypothesis based on a neutralization reaction and to use time of salt heating to decomposition temperature as an ID definition in their model. The trend of WFNA leading to shorter IDs than RFNA would have been the opposite if oxidation were the dominant reaction [9]. Oxidation was proven to occur in the preignition stage based on the intermediate species found, but the neutralization reaction is more dominant.

In the case of monothiocarbonohydrazones, ID had previously been found to be a function of electrophilic or electron withdrawing substitution in the phenyl ring due to exothermic nitration. Because bisderivatives have two phenyl rings instead of one, one would expect the bisderivatives to have shorter ignition delays than their monoanalogs. This was not the case, however, so it was suggested that nitration was not the most prominent preignition reaction.

### **2.2.2 Surface Reactions**

Bernard et al. researched surface reactions contributing to the hypergolic ignition of hybrid propellants [11]. They used various fuel powders, primarily p-phenylenediamine and lithium hydride, with WFNA and dinitrogen tetroxide (NTO) as oxidizers. Oxidizer chemical formulae are  $\text{HNO}_3$  and  $\text{N}_2\text{O}_4$ , respectively. Drop tests resulted in observation of crystals thought to be salts on fuel particle surfaces. This observation led to a hypothesis of instantaneous nuclei formation and two-dimensional growth followed by a surface reaction controlling ignition delay. In order to further understand this surface reaction, they varied the water content in their nitric acid to find the order of reaction with respect to  $\text{HNO}_3$ . The role of oxidizer concentration will be discussed further in Section 2.4.6. They were also able to determine that surface reactions occur in the adsorbed phase on the fuel surface.

Bernard et al. also sought to determine the active component in nucleus formation on the fuel particle surface. It would either be the oxidizers themselves ( $\text{HNO}_3$  or  $\text{N}_2\text{O}_4$ ) or their corresponding acid ions ( $\text{NO}^+$  or  $\text{NO}_2^+$ , respectively). To examine the WFNA case,  $\text{NO}_2^+$

concentration was varied using salt additions ( $\text{KNO}_3$  and  $\text{NO}_2\text{ClO}_4$ ) to the WFNA to shift the autodissociation equilibrium. They determined that the ions ( $\text{NO}^+$  or  $\text{NO}_2^+$ ) were the active component.

### 2.3 Ignition of Amine-Boranes

Multiple pieces of literature have used qualitative observation as well as dedicated scientific study to describe and better understand the hypergolic hybrid ignition process. Pfeil's work focused on amine-based materials as fuels, specifically ethylenediamine bisborane (EDBB) and ammonia borane (AB) [1, 2, 4]. Amines are bases involving one nitrogen atom and three of some other chemical, following the pattern  $\text{NR}_3$  [1]. They have a lone pair of electrons and can readily accept protons ( $\text{H}^+$ ) from acid. The ensuing Lewis acid-base (neutralization) reaction results in heat generation, formation of a salt, and formation of a strong oxidant. This heat release accelerates this reaction as well as the fuel-oxidizer reaction. This runaway eventually leads to ignition. Pfeil also discussed the process responsible for the hypergolic ignition of metal hydrides, but there has not been enough study in this area for this process to be verified. Metal hydrides are similar to salts, so it was suggested that they could react with a strong acid in a similar manner. The positively charged acid could potentially cause the hydride to be removed from the metal, and the ensuing reaction would produce heat and hydrogen. This hydrogen would then react with the oxidizer, and the reaction would runaway to the point of ignition.

Borane ( $\text{BH}_3^+$ ) adducts to amine-based materials have been studied as a way to improve their ignition delay [1, 2]. Although there was no previous work in this area, an explanation of the shorter ignition delays observed was proposed. Borane functions as an acid in its bond to amine. When a stronger acid comes into contact with the amine-borane, it may replace the borane and react with the amine by itself in the typical acid-base reaction previously described. The borane which was replaced would simultaneously react in the gas phase with the strong oxidizer due to borane's reactivity and pyrophoric nature. This would provide an additional mode of heat generation which would accelerate the reaction even more and eventually lead to the ignition of the borane gas.

Pfeil et. al described the ignition and subsequent combustion of EDBB loose powder and WFNA during ignition delay tests using droplets of WFNA [2]. The first emission of light (green in this case) is considered ignition. This green flame then grew to surround the powder and

indicated the presence of boron combustion, indicating the role of borane groups in the initial reaction. Yellow flames were later observed, indicating carbon combustion. However, the delayed appearance of yellow emissions suggests that carbon was present but did not contribute to the ignition process. This sequence of events is shown in Figure 2.1.

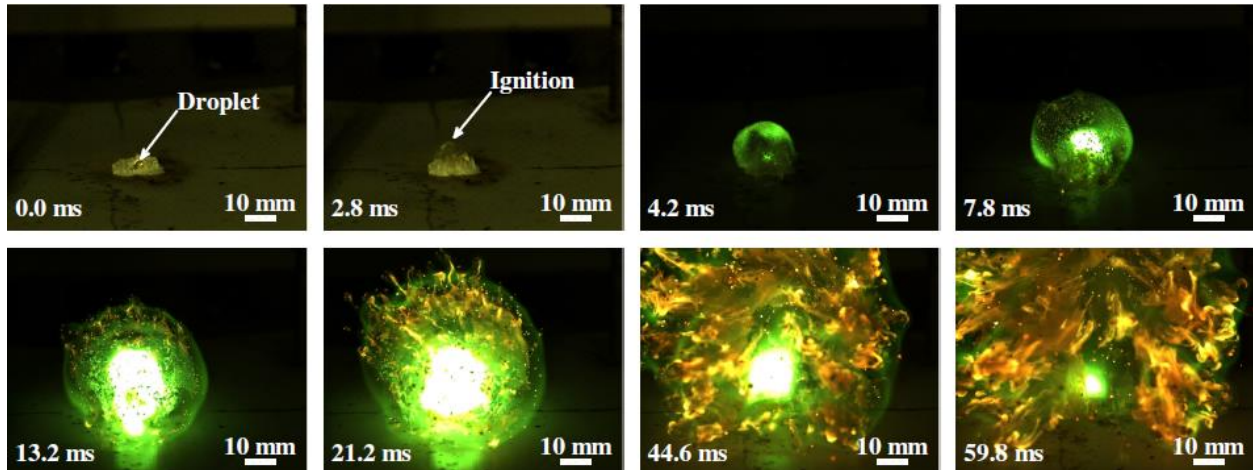


Figure 2.1. Ignition of EDBB powder with WFNA. (Image from [2].)

Pfeil et. al also noted the behavior of pressed EDBB pellets with WFNA. The following “violent reaction” is shown in Figure 2.2. Upon hitting the pellet, the droplet spread across the surface, and WFNA began to bubble as it reacted with the EDBB. When a large enough amount of gaseous products were produced, they expelled the WFNA off the surface of the pellet and the reaction was quenched due to the resulting rapid depressurization. They postulated that this WFNA expulsion was due to ignition between the WFNA layer and the pellet surface, because it matched the ignition delay time of the loose powder. Sometimes there would be another ignition event if the expelled oxidizer fell back on the pellet. Because of this effect, they postulated that this type of behavior would lead to short ignition delays in an actual rocket motor, because the fuel surface would constantly be getting hit with WFNA. Similar behavior to the pressed pellet was noted for the sanded pellet but on an even quicker time scale.

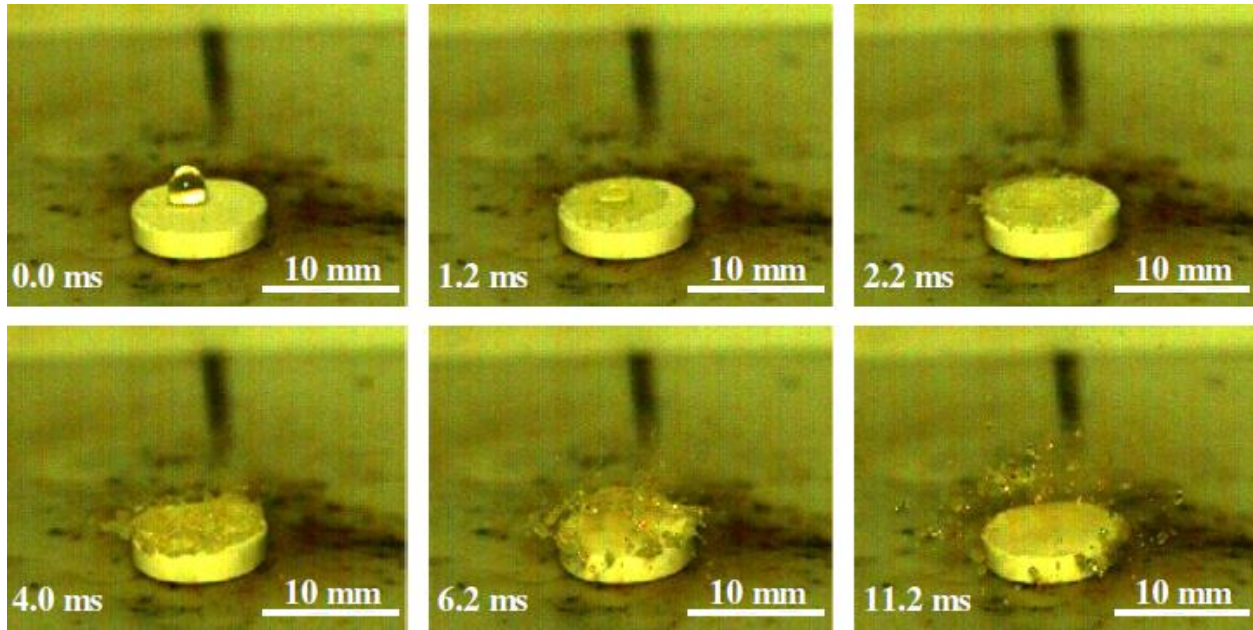


Figure 2.2. Violent reaction of EDBB pellet with WFNA. (Image from [2].)

## 2.4 Factors Affecting Ignition Delay

### 2.4.1 Compactness

Munjal and Parvatiyar utilized a cup test to measure IDs in aniline formaldehyde with fuming nitric acid (assumed to be WFNA based on density given) [12]. They pressed fuel grains at 6720, 8960, 11200, and 13440 lb over 3.143 in<sup>2</sup> of fuel and did not place powder on the surface of their grains after pressing them. They found that increasing the pressure, and thus increasing fuel density, increased ignition delay due to the decrease in acid diffusion rate and decrease in exposed surface area. This was also observed by Jain et al. with hydrazone and RFNA [13].

On a related note, Munjal and Parvatiyar found that up to a certain oxidizer to fuel ratio (O/F), increased surface area, as would be the result of less pressure applied, led to decreased ignition delays [12]. Increasing surface area decreasing ignition delay makes sense considering that hypergolic ignition is primarily driven by surface reactions immediately after fuel-oxidizer contact as discussed in Section 2.2.2. Jain et al. noted that hypergolicity of a fuel in powder form does not necessarily lead to hypergolicity in pellet form [14], an observation likely due to a difference in exposed surface area. Pfeil et al. compared cut and sanded pellets to elucidate the effect of different surface types [4]. They found that sanding the surface of the pellets, and thus

exposing more surface area, led to drastically shorter ignition delays than cut surfaces by factors of up to 16.5. They were also able to measure the difference in surface feature depth using a Hirox microscope. In addition to removing binder and exposing more fuel, they concluded that sanding also reduces ignition delay by deepening these surface features, allowing the fuel-oxidizer reactions to be partially confined. This leads to local pressurization and faster reaction. A comparison of powder versus pellet ignition behavior is provided in Section 2.3.

#### 2.4.2 Fuel Particle Diameter

Bernard et al. found ID ( $\tau$ ) to be proportional to the square root of initial fuel particle diameter ( $d_o$ ) as in Eq. (2.1). [11]. This relationship was proposed to be universal, because it applied to eight different systems tested.

$$\tau \propto \sqrt{d_o} \quad (2.1)$$

However, Pfeil et al. sieved their material to get more uniform sizing and got mixed results [4]. Several amine-boranes and amines were tested, but, in most cases, the change in ID between the sieved material and the as-received material was within one standard deviation of the measured ID of the sieved material. Therefore, it was concluded that sieving did not significantly affect ID. Perhaps the as-received material was already similarly sized to the sieved material. In contrast to the other materials tested, AB did appear strongly affected by sieving, since the difference in ignition delays for sieved and unsieved material differed by an order of magnitude. Baier et. al also observed shorter IDs for smaller particle sizes of AB in powder form, but this effect was not observed when the AB was pressed into pellets [6].

#### 2.4.3 Temperature

Munjal and Parvatiyar took ID measurements at 10°C, 15°C, 18°C, 20°C, and 25°C [12]. The fuels tested included aniline formaldehyde, o- and m- toluidine formaldehyde, and o-anisidine formaldehyde. All were in powder form, and all were tested in a 1:1 O/F with fuming nitric acid except for aniline formaldehyde which was tested at 1:2 O/F. Increasing temperature caused ID to decrease, likely due to temperature causing increased reaction rate. In some cases, the effect of

temperature was drastic such that ignition delay was reduced 50% or more between 10°C and 25°C.

Kulkarni and Panda noted that fuel particles have low thermal conductivity, so with the preignition reactions occurring on the surface of the fuel particle, the heat generated by said reactions does not quickly reach the interior of the particle [15]. Therefore, they studied twenty-one different solid compounds proven to be hypergolic with RFNA to investigate if thermal decomposition of the fuel has a strong impact on ID. However, they determined that hypergolicity with RFNA is not influenced by the fuel's thermal reaction or degradation.

#### **2.4.4 Pressure**

It was briefly mentioned by Bernard et al. that pressure could theoretically affect ignition delay [11], but this parameter was not included in their study. Mullins studied fuel ignition when injected into a stream of hot air [16], and Anderson et al. made a mathematical model for the hypergolic ignition of solid fuels with gaseous oxidizers [17]. Both arrived at the same expression for pressure-dependence of ignition delay given in Eq. (2.2) where  $m$  is the pressure exponent and  $K$  is a constant.

$$\tau = \frac{K}{p^m} \quad (2.2)$$

This correlation was experimentally verified by Spengler et al. using furfuryl alcohol and nitric acid [18]. Benhidjeb-Carayon et al. sought to determine if this relationship also held for MON-25 (75 wt.% NTO and 25 wt.% nitric oxide) and NTO with various hypergolic fuels [8]. They confirmed that increasing pressure drastically decreases ID, up to almost 3 times for NTO and up to 19 times for MON-25. Tests were performed in a nitrogen environment at 30, 50, and 80 psia.

#### **2.4.5 Amount or Ratio**

Munjal and Parvatiyar found that different fuels have different corresponding critical amounts of fuel for a given amount of oxidizer that lead to minimum IDs [12]. They experimentally identified these critical amounts by performing ignition delay tests on 0.2 g, 0.3 g, 0.5 g, 1.0 g, and

1.5 g of each formaldehyde fuel with 1.0 cm<sup>3</sup> of WFNA to find which amount produced the lowest delay for each fuel. Jain et al. performed a very similar study with hydrazine fuels and RFNA [13]. They found that the minimum ignition delay mostly occurred at a mixture ratio near stoichiometric. This is not surprising, because stoichiometric ratio should result in the most heat generation from the fuel-oxidizer reaction. There were some exceptions, however. Hydroxyl- and methoxybenzaldehyde phenylhydrazones and dimethylhydrazones exhibited minimum ignition delays with greater oxidizer concentration (less fuel) than stoichiometric due to bonded oxygen in the fuels. While ID was the main concern of the study, it was also noted that at the ratios producing the shortest IDs, resulting flame consistency and reproducibility of measured ID were excellent in most cases.

Additionally, O/F has a theoretical effect on specific impulse [4]. This is illustrated in Figure 2.3 for several different hypergolic fuels with inhibited red fuming nitric acid containing 83.4% HNO<sub>3</sub> (IRFNA IIIA). One advantage of amine-boranes over other hypergolic fuels is that they have two performance peaks. This means that they maintain their performance even amid transients, such as ignition, shutdown, and throttling.

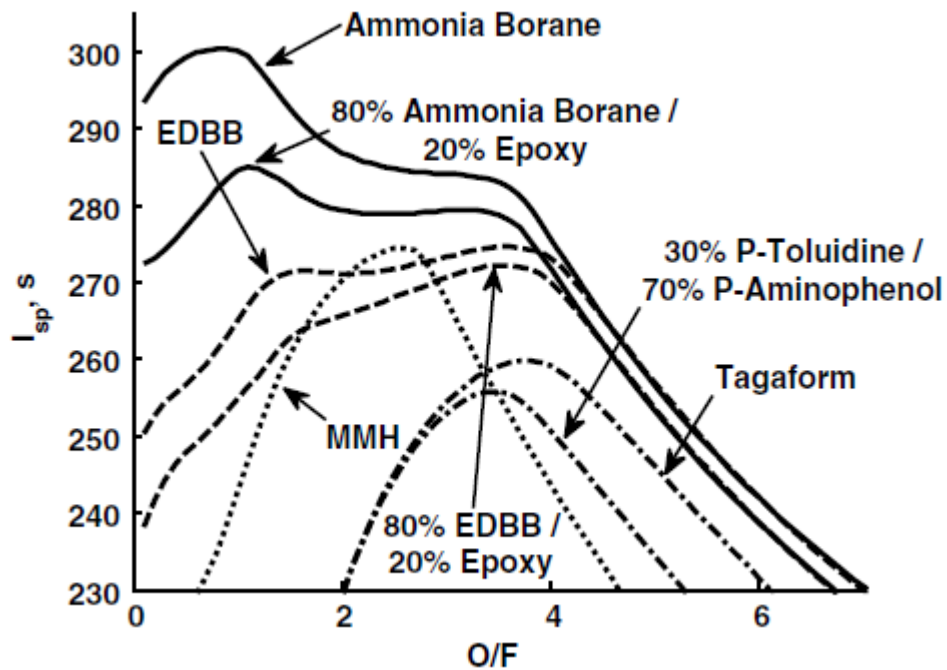


Figure 2.3. Specific impulse of hypergolic fuels with IRFNA IIIA. (Image from [4].)

#### 2.4.6 Oxidizer Concentration

Bernard et al. varied water content in their nitric acid to determine the effect on ID and order of surface reaction [11]. Not surprisingly, they found that decreasing HNO<sub>3</sub> concentration (by increasing water content) lengthened ID. For weaker acid concentrations, they found the relationship given in Eq. (2.3) where  $\beta$  is the order of reaction and  $C_{HNO_3}$  is the concentration of nitric acid.

$$\tau \propto C_{HNO_3}^{-\beta} \quad (2.3)$$

Similarly, Anderson et al. found the theoretical correlation in Eq. (2.4) for reaction-controlled cases where  $C_{ox}$  is the concentration of the oxidizer (whichever oxidizer that may be) and  $\gamma$  is the order of reaction [17].

$$\tau \propto C_{ox}^{-2\gamma} \quad (2.4)$$

Jain et al. found that, in addition to water diluting an acid and thus lengthening IDs, IDs are also lengthened with increased NO<sub>2</sub> concentration even when the same amount of water is present [13]. The explanation for both of these observations, however, is that a higher concentration of either water or NO<sub>2</sub> effectively dilutes the HNO<sub>3</sub> needed for the exothermic neutralization reaction leading to ignition. As one would expect, pure nitric acid led to the shortest IDs.

There are some cases, however, when higher oxidizer concentration actually interferes with ignition. Baier et al. were unable to ignite pure AB pellets using WFNA but reliably ignited them with 70% HNO<sub>3</sub> [19]. This is discussed more in Section 4.2.3.

#### 2.4.7 Binder

The fuel binder used in a fuel grain or pellet has a significant effect on ID. Pfeil et al. used paraffin, RTV silicon, and epoxy binders [4]. Epoxy resulted in the shortest ID with RTV silicon slightly behind. However, paraffin produced IDs about six times as long as epoxy. The comparatively poor performance of paraffin is likely due to the lack of structural integrity thus

allowing it to remain coating the fuel and thus preventing exposure to the oxidizer. Cortopassi and Boyer attempted to ignite a wax matrix containing hypergolic solid additives with MON-3, but this was unsuccessful [20]. They used SP7 wax and 50 wt.% or 25 wt.% solids loading of seven different fuels (sodium amide, sodium cyanoborohydride, lithium amide, triaminoguanidinium azotetrazolate, trimethylamine borane complex, borane tert-butylamine complex, and AB), but none of them hypergolically ignited. Loose powder was even added as a surface coating in some cases in an attempt to facilitate ignition, but this was to no avail. From these results, it was concluded that even at high solids loadings, the wax matrix greatly hinders the fuel-oxidizer reaction.

Jain et al. found that binder has a large influence on ID, as well [14]. They found that casting fuels in carboxyl or hydroxyl terminated polybutadiene (HTPB) significantly lengthened IDs of multiple fuels compared to the same fuels in powder form. They also cast fuels in newly synthesized epoxies which resulted in shorter IDs than those achieved with the polymer binders and better structural characteristics. They concluded from their results that the binder used plays an important role in the ignition characteristics of a hypergolic hybrid system. The role of binder is discussed extensively in Sec. 4.2.3.

#### **2.4.8 Additives**

Because ignition catalysts are often used in liquid-liquid hypergolic systems and non-hypergolic bipropellants, Munjal and Parvatiyar sought to determine if they could improve the ignition performance of hypergolic hybrid systems [12]. Multiple ammonium, potassium, and vanadium salts were attempted, the most successful being ammonium vanadate, ammonium dichromate, and vanadium pentoxide. These additives were added to the nitric acid at a concentration of 4.5 g in 100 cm<sup>3</sup> of acid. While the exact cause was unclear, they did lower ID but did not contribute to the heat of combustion and would not affect  $I_{sp}$ .

Jain et al. explored the effect of adding metals to hypergolic propellants [10]. They were able to decrease IDs in systems with longer delays as well as hypergolically ignite fuels that were previously non-hypergolic with WFNA. Magnesium powder was the metal addition primarily used, but the same phenomenon was also observed with zinc, iron, and copper. This synergistic hypergolicity is likely mostly due to the metal and oxidizer reacting exothermically in addition to the organic fuel-oxidizer reaction resulting in increased overall exothermicity. The magnesium-

WFNA reaction also contributes to the organic fuel-WFNA reaction by producing magnesium nitrate as an intermediate. The magnesium nitrate may facilitate nitration by dehydrating the system. In addition, the magnesium nitrate produces oxygen when it decomposes, thus contributing to the oxidation of the organic fuel.

Jain et al. explored synergistic hypergolicity further in the form of fuel pellets [14]. They observed minimum IDs between 40% and 50% magnesium content. Additional magnesium content lowered the ID even further in some cases, but this came at an unacceptable cost of decreased structural integrity. However, this reduced structural performance was attributed to porosity due to insufficient fuel melting during the melt-casting of their pellets. While they did not offer this possibility, it is possible that a different casting method would ameliorate this effect. However, they established earlier that melt-casting reduced ID compared to traditional casting, so the possibility of changing casting methods to include more magnesium may not be worthwhile.

As part of Bernard et al.'s study of surface reactions, 1% ethoxylated lauryl alcohol was added to the furfuraldehyde in order to study the effect of a surface active agent. The average ID of this mixture with WFNA was unaffected, but the addition did result in a narrower distribution of results compared to plain furfuraldehyde with WFNA [11].

## **2.5 Ignition in Motor Environment**

Ignition behavior and factors of hypergolic fuels in powder or pellet form are obviously relevant to hypergolic hybrid motor grain ignition, but there are some additional factors that must also be addressed. In real motors, ID is also impacted by injection velocity and degree of oxidizer atomization [12].

Pfeil found oxidizer impingement and fuel grain conditions to be important factors in motor grain ignition [1]. Eight of the nine EDDB grains tested ignited hypergolically with WFNA without issue. However, one of the tests had almost double the oxidizer flux of the other tests and did not ignite. This grain had also been used previously. It had been cleaned out to remove burnt material and reacted material, but it was not in its original pristine condition. It is likely that one or both of these factors contributed to the lack of ignition. Pfeil also had a test in which the grain ignited but then quenched when the oxidizer flow rate was suddenly increased. This confirms that steadiness of the oxidizer flux is important for ignition and continued burning.

## 2.6 Conclusion

Hypergolic hybrid systems offer many advantages over liquid hypergolic systems as well as non-hypergolic systems due to their simplicity, reliability, storability, and ability to be restarted and throttled. However, hypergolic hybrid systems have typically had longer ignition delays or other performance drawbacks compared to their liquid hypergol counterparts, or they had problems with toxicity or pyrophoricity. Therefore, there has been study into the mechanisms that drive hypergolic ignition so that fuels can be optimized for this process. It has been found that nitration, oxidation, and neutralization are the main reactions contributing to the phenomenon with neutralization being the most impactful.

Factors affecting ignition delay have also been studied. This allows shorter ignition delays for given fuels to be achieved, exposes the aspects of testing that should be controlled to get consistent results, and can be used to verify hypotheses related to the ignition process. Reduced ignition delays are typically achieved with less compact fuel, smaller initial fuel particle sizes, increased temperature, high pressure, and high oxidizer concentration. Ignition delays are typically the shortest near stoichiometric ratio, although there are some exceptions for which a fuel-lean reaction results in shorter ignition delays. Additionally, additives can be added to the fuel or the oxidizer. In the case of pellets, epoxy binders are better suited for hypergolic ignition than paraffin or other waxes. In the case of actual motor grains, the oxidizer flow rate is another consideration. Sudden increases in oxidizer flux can quench a reaction, and too much initial oxidizer flux will result in not having any ignition to begin with. Multiple groups have conducted small-scale motor testing and obtained performance values such as  $I_{sp}$ , characteristic velocity ( $C^*$ ), and thrust, but that is beyond the scope of this review which emphasized the ignition process itself.

### 3. METHODS

#### 3.1 Fuel Powder

Fuel pellets were made using AB powder and Envirotext Lite epoxy. The AB powder was prepared at Purdue University's H. C. Brown Center for Borane Research according to a water-promoted synthesis method devised by Ramachandran and Kulkarni [21]. Before forming the pellets, the AB powder was dried in an oven at 60°C for 3 days. Drying the powder turned out to be unnecessary for achieving consistent and timely ignition. However, it made for a constant starting point for material used in experiments performed at different times of year in varying ambient humidities. By extrapolating reaction onset data from higher temperatures, Rassat et al. determined that AB should be stable for about 5.5 days at 60°C [22], so the 3-day drying period was deemed acceptable. Boron nuclear magnetic resonance (NMR) spectroscopy was performed on samples of both dried and as-received powder, and it confirmed that there was no dehydrogenation of the AB as a result of the drying process. Additionally, Fourier-transform infrared (FTIR) spectroscopy was performed and showed identical peaks for the dried and as-received powder. Samples were tested for purity based on hydrogen production from reaction with hydrochloric acid (HCl). The dried AB powder was 89.5% pure compared to 93.0% for as-received powder taken directly from the bulk storage container. Based on the work of Bowden et. al, it is possible that some of the AB sublimed or transitioned to a more mobile phase during the drying process in the oven [23]. Hydrogen generation from heating would have only come after these steps. No hydrogen generation or AB sublimation were observed using mass spectroscopy, but the time needed for this to potentially occur at 60 °C exceeded the length of time the mass spectrometer could be run. Zhang et al. found that pre-heating AB for 2-4 hours at 80 °C (shorter duration but more intense than the drying procedure presented here) shortens the time needed for hydrogen release [24], but it is unclear whether this would matter for time scales as short as those of hypergolic ignition. In the work presented here, a longer average ID was observed for pellets made from powder dried only in the dry box (described below) compared to those made from oven-dried powder (10.8 ms and 6.91 ms, respectively for unsanded 80% AB pellets). However, data for non-oven-dried material was only taken at one test condition on one test day, so it may not be conclusive.

After being removed from the oven, the powder was then placed in a dry box kept at 10-13% relative humidity (RH). The dry box used 98% phosphorus pentoxide ( $P_2O_5$ ) powder and Drierite calcium sulfate as desiccants.

### 3.2 Fuel Pellets

For the pressed pellets, the AB and epoxy were first thoroughly hand-mixed. The individual pellets were then pressed in a 1 cm die on a Carver press for 3 minutes at 81.9 MPa. The equipment described is shown in Figure 3.1. For the cast pellets, the AB and epoxy were hand-mixed as before. Then individual pellets were formed by putting small amounts of the AB-epoxy mixture in 1 cm diameter sections of plastic straw. All pellets were then left to cure for at least 72 hours in the dry box. The sanded pellets were individually sanded with 100 grit sandpaper, and excess powder that formed at the surface was brushed away gently with a paintbrush. With the exception of the pre-sanded pellets used in the humid aging study discussed in Section 4.3, all sanded pellets were stored unsanded and were not sanded until immediately before each test run.



Figure 3.1. Equipment used for fuel pellet preparation: oven (left), dry box (center), and Carver press (right).

### 3.3 Ignition Delay Tests

All tests were performed at atmospheric conditions and used white fuming nitric acid (WFNA) (Sigma Aldrich, Lot # BCBK8646V) as the oxidizer. WFNA was transferred in an argon environment from its original bottle into smaller individual vials for each test day. Details of this procedure can be found in Appendix A. This minimized the contamination of WFNA by moisture

in the air. WFNA purity was found to be 94.5% by mass based on measured WFNA density and theoretical densities for WFNA and water.

The droplet test apparatus is shown in Figure 3.2. The syringe (Hamilton #1710, gas tight 100  $\mu\text{L}$ ) is held by a polytetrafluoroethylene (PTFE) arm. This arm can be slid up and down the vertical post to adjust initial droplet height. The average diameter of the WFNA droplet released from the syringe was 2.9 mm. The base is covered by two stainless steel plates. The bottom plate is solid, and the top plate has a hole where the pellet sits. This ensures that the pellet is in the same position for each test, thus guaranteeing that the droplet lands on the pellet each time. The apparatus was illuminated using a portable halogen work light. The extra lighting was required due to the short exposure times being used. Tests were recorded with a Phantom v5.1 high speed color camera at 5,000 frames per second. Details of this procedure can be found in Appendix B.

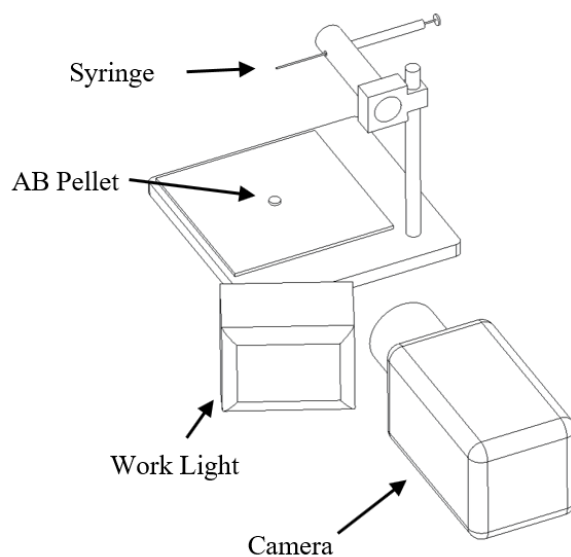


Figure 3.2. Droplet test configuration.

The ID was found by subtracting the frame number of droplet impact from the frame number of the very first visible light emission and dividing by the frame rate. Due to the frame rate of 5,000 frames per second, 0.2 ms passed between each frame. Therefore, since two events (impact and ignition) were used for each data point calculation, the maximum uncertainty of each data point is 0.4 ms.

An example sequence of events is displayed in Figure 3.3. Additional data was also collected using the frame of the first light leading to eventual sustained ignition of the whole pellet. This will hereafter be referred to as “main ignition”. This was often the same as the initial ignition or very close, but sometimes it was different if the initial ignition occurred off the pellet or if the initial flame extinguished before spreading. A test in which initial and main ignition events were different is shown in Figure 3.4. To get a comparison of these two different ID interpretations, only tests in which the pellet eventually fully ignited were considered.

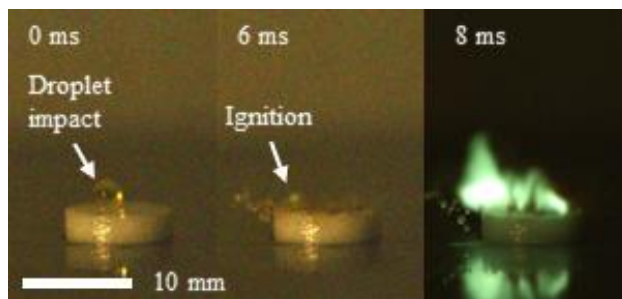


Figure 3.3. Image sequence of ignition delay test of 80% AB pellet with WFNA.

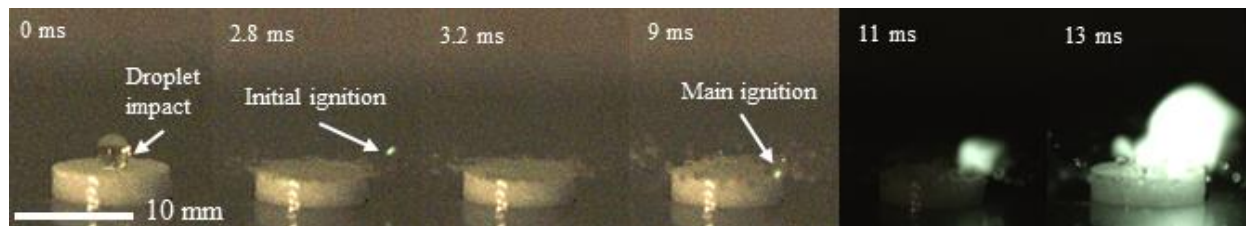


Figure 3.4. Image sequence of test with separate initial and main ignitions.

Analysis of variance (ANOVA) was considered for interpreting results of the droplet velocity (Section 4.1) and storage humidity tests (Section 4.3), because their trends were not visually obvious. However, the only case where ANOVA could actually be used was for the unsanded case of varying droplet velocity, because this is the only case that met the normal distribution criteria required for ANOVA to be relevant. The normalcy of the data was determined by plotting Z score versus ID for a given test condition and checking for linearity. An example of a normal distribution is shown in Figure 3.5. This is for initial ignition of unsanded 80% AB pellets with a WFNA droplet impact velocity of 117 cm/s. ANOVA could be applied when all the test

conditions to be compared (e.g. all the droplet velocities) produced roughly linear Z score versus ID plots.

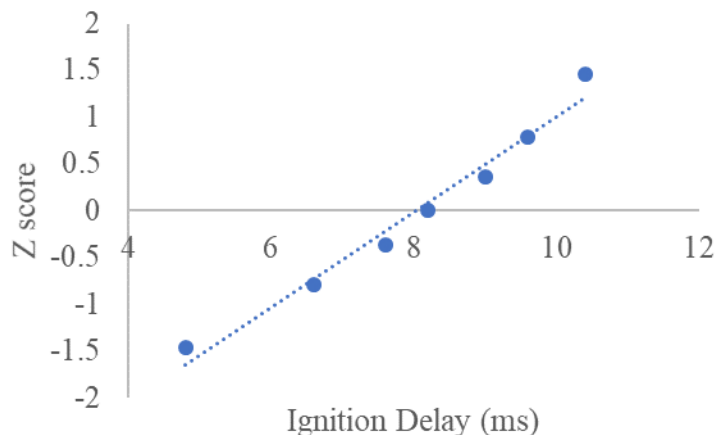


Figure 3.5. Example of normal distribution to which ANOVA was applied.

### 3.4 Wetting Contact Angle Tests

Wetting contact angles between WFNA and various binders were measured by placing individual droplets of WFNA on binder samples with a syringe. Images of the droplets on the samples were taken with a Nikon D500 DSLR camera using a K2 lens with a CF-3 objective (92-125 mm working distance). The binder samples were backlit using an LED light box. Because some of the samples were expected to become wetted very quickly, the camera was used in video mode to capture the initial contact angle in addition to the steady-state contact angle. The initial contact angle was taken using the first frame where a droplet shape was clearly defined and separated from the syringe tip. The steady-state contact angle was taken using the very end of the video (several seconds after oxidizer contact). Images were analyzed for contact angle using the ImageJ plugin, DropSnake. A sample image analyzed for contact angle is given in Figure 3.6. Average contact angles were found by averaging the left and right contact angles for all the samples of a given binder.

The binders tested matched those used by Pfeil in his ignition delay tests of EDBB [1]. Binders tested include Envirotex Lite Epoxy, HTPB, R-45, paraffin wax, and Permatex High-Temp Red RTV Silicone. The HTPB and R-45 were both mixed with 5.9 wt.% dioctyl adipate (DOA), and 7.7 wt.% isophorone diisocyanate (IDPI). Both mixtures were cured at 60 °C for 5 days. The epoxy

was made with equal parts resin and hardener and cured at ambient conditions for 3 days. The RTV cured for over 1 day at ambient conditions. The paraffin was melted and cast but did not need to cure. Binder samples were made by casting the binders in small pans and then cutting them into smaller pieces after they were done curing.

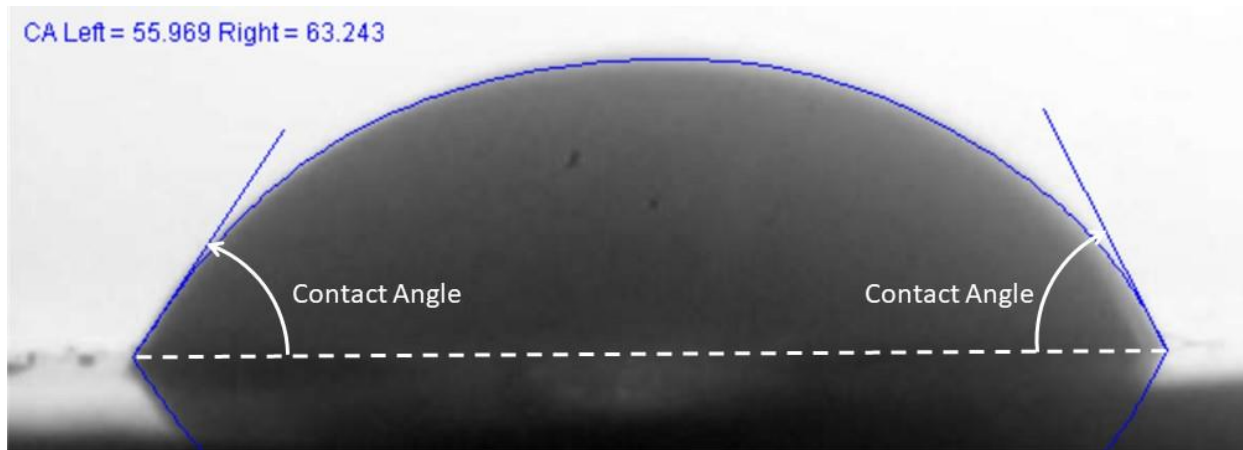


Figure 3.6. Sample image used for initial contact angle measurement of WFNA on RTV.

## 4. RESULTS

### 4.1 Droplet Impact Velocity

Droplet impact velocity is an important factor for ID in liquid hypergolic systems due to its role in the mixing of the fuel and oxidizer fluids. In liquid hypergol injectors, gases formed from propellant contact can push the propellant streams apart, hindering mixing. Therefore, it is advantageous to make liquid hypergol impingement velocities sufficiently high in order to make the droplet breakup time shorter than the gas evolution time [25]. Since the oxidizer does not mix with the solid fuel in a hybrid system, however, it was not clear if impact velocity would still be influential. The effect of droplet impact velocity on ID was studied by varying the height of the WFNA syringe above the pellet. The syringe height was set to 38.1 mm (1.5 in), 76.2 mm (3 in), and 127 mm (5 in) to achieve impact velocities of 76 cm/s, 117 cm/s, and 148 cm/s, respectively. Velocities were calculated by video analysis. The results for 80% AB pellets are given in the box and whisker plot in Figure 4.1 and numerically in Table 4.1. For a given box and whisker, the top and bottom dashes represent upper and lower extremes, respectively. The top and bottom of the box represent upper and lower quartiles, respectively. The middle line is the median value, and the “X” marks the mean. The circles are outliers.

For unsanded pellets, greater impact velocities decreased ignition delay with >99% confidence based on ANOVA for both initial and main ignition. ID of sanded pellets appears to be the shortest for the middle droplet velocity of 117 cm/s, but with such large variation, this is not conclusive. It is also worth noting that sanding the pellets resulted in greater deviation in ID and often higher ID values. This held true for other solids loadings, as well. The greater deviation was to be expected due to the inherently inconsistent nature of sanding and brushing. The higher ID values, however, were surprising, since sanding the pellets exposes more fuel surface area and deepens surface features which may allow for local pressurization [1]. However, this explanation came about from a test campaign in which the excess powder was not brushed off the sanded pellets. It is possible that the shorter IDs observed for sanded, unbrushed pellets was due more to reaction with the loose powder on top rather than the pellet itself. It is also possible that the removal of epoxy has an effect that overrides the effect of increased surface area and potential pressurized regions. The role of epoxy is discussed more in Section 4.2.3.

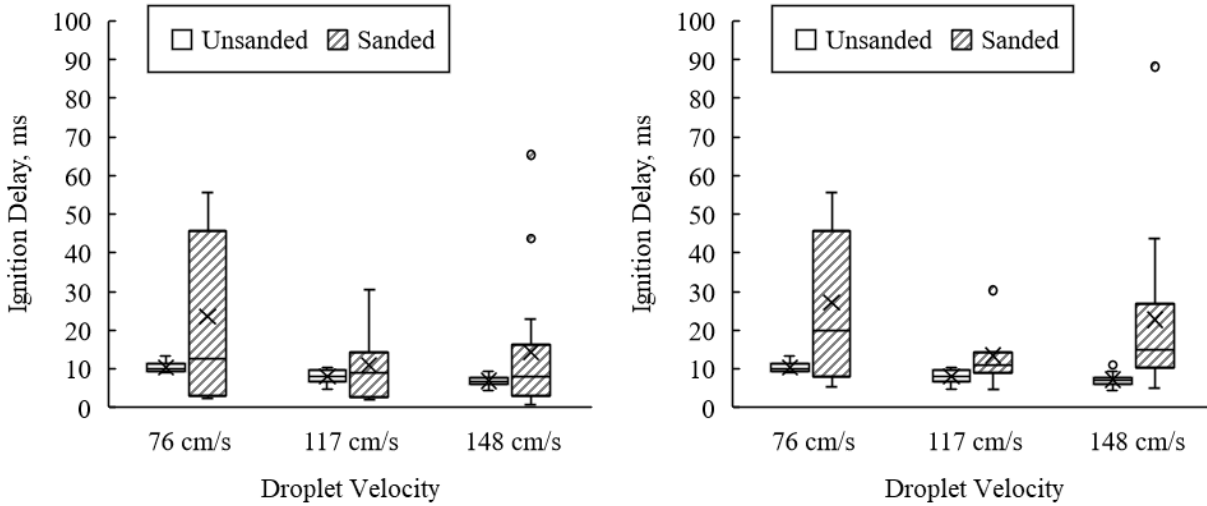


Figure 4.1. Ignition delay of 80% AB pellets as a function of droplet impact velocity based on initial ignition (left) and main ignition (right).

Table 4.1. Numerical results of varying droplet impact velocity.

Droplet Velocity, cm/s	Surface	Initial ID, ms	Standard Deviation, ms	Main ID, ms	Standard Deviation, ms	# Tests
76	Unsanded	10.43	1.32	10.43	1.32	7
76	Sanded	23.51	20.99	27.14	18.23	7
117	Unsanded	8.03	1.76	8.03	1.76	7
117	Sanded	10.97	9.22	13.49	7.52	7
148	Unsanded	6.93	1.31	7.16	1.59	14
148	Sanded	14.40	17.78	22.73	21.03	14

## 4.2 Solids Loading

### 4.2.1 AB Pellet Results

The results of varying the solids loading of the pellets are given in Figure 4.2 and Table 4.2. The percentage on the x-axis is the percent AB by mass with the rest of the mass being epoxy. These tests were performed at a syringe height of 127 mm (5 in) to remain consistent with Pfeil [1] so that a comparison may be made with EDBB. It should be noted that because the 30% AB pellets could not be pressed in the same manner as the others due to their excess of epoxy, they were more porous and had irregularly shaped surfaces. Multiple groups have found that higher fuel pellet density for a given fuel relates to longer IDs, because more compact pellets have less

exposed surface area and slower oxidizer diffusion [12-14]. Therefore, it can be assumed that the low average ID at 30% solids loading is a result of the difference in pellet preparation rather than the AB amount itself. Despite this caveat, this data point is still valuable in its illustration that AB can result in hypergolic ignition even in small amounts relative to the binder.

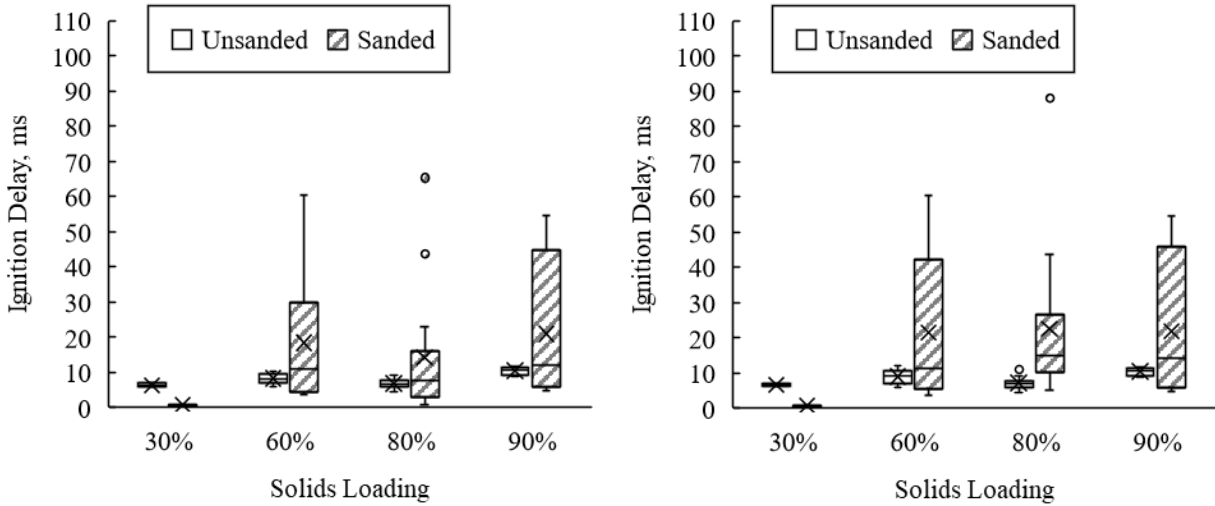


Figure 4.2. Ignition delay of AB pellets as a function of solids loading based on initial ignition (left) and main ignition (right).\*

Table 4.2. Numerical results of varying solids loading.

Solids Loading	Surface	Initial ID, ms	Standard Deviation, ms	Main ID, ms	Standard Deviation, ms	# Tests
30%	Unsanded	6.40*	0.45	6.60	0.28	4
30%	Sanded	0.85*	0.17	0.85	0.17	4
60%	Unsanded	8.23	1.39	9.03	1.93	6
60%	Sanded	18.50	19.55	21.60	20.36	6
80%	Unsanded	6.93	1.31	7.16	1.59	14
80%	Sanded	14.40	17.78	22.73	21.03	14
90%	Unsanded	10.55	1.09	10.55	1.09	4
90%	Sanded	20.95	19.89	22.00	19.67	4

\* AB pellets with 30% solids loading were cast instead of pressed due to the large amount of epoxy that would be lost if pressed in a die.

Of the pressed pellets, 80% solids loading appears to minimize ID, although results are comparable to that of 60% and 90% solids loadings. It should be noted, however, that even the longer IDs observed in this experiment may be short enough for use in hybrid systems, because the risk of hard starts is lower than in liquid systems.

Neat pellets (100% AB and no binder) were tested as well. When successfully ignited, their IDs were slightly longer than those of the 80% AB pellets, but their ignition was not reliable. In addition, they failed to ignite when made from powder kept at ambient conditions, and they only sometimes ignited when made from dried powder. The surprising result that pellets comprised of 80% AB ignited faster and much more reliably than pellets made from 100% AB prompted a closer look at the role of the epoxy in pellet ignition (Section 4.2.3).

Pellets were also tested without brushing away the excess powder after sanding. This demonstrated that the other results are conservative representations of ID. Pfeil et al. observed ID reductions of factors up to 16.5 by sanding and not brushing pellets compared to pellets with cut surfaces [4]. In a real motor grain, the surface would be sanded but not brushed, so it is expected that the ID would be shorter than those of the sanded pellets presented in Figures 4.1 and 4.2. Not brushing the sanded pellets also allowed for neat AB pellet data to be collected as it allowed the pellets to be ignited more reliably. The results of sanding the pellets but not brushing them are given in Figure 4.3 and Table 4.3. All average initial IDs for this surface condition were below 2.5 ms and less than 1 ms for 60% and 80% solids loadings. Besides the neat pellets, even the main IDs observed were extremely short at 0.70 ms, 1.07 ms, and 2.20 ms for 60%, 80%, and 90% solids loadings, respectively. While these are all short IDs, the fact that they decrease with decreasing AB content again underlines the role of epoxy. There is a much greater difference between the first ignition and main ignition for the neat pellets than for any other sample condition tested. This is likely due to the violent reaction phenomenon discussed in Sections 2.3, 4.2.2, and 4.2.3.

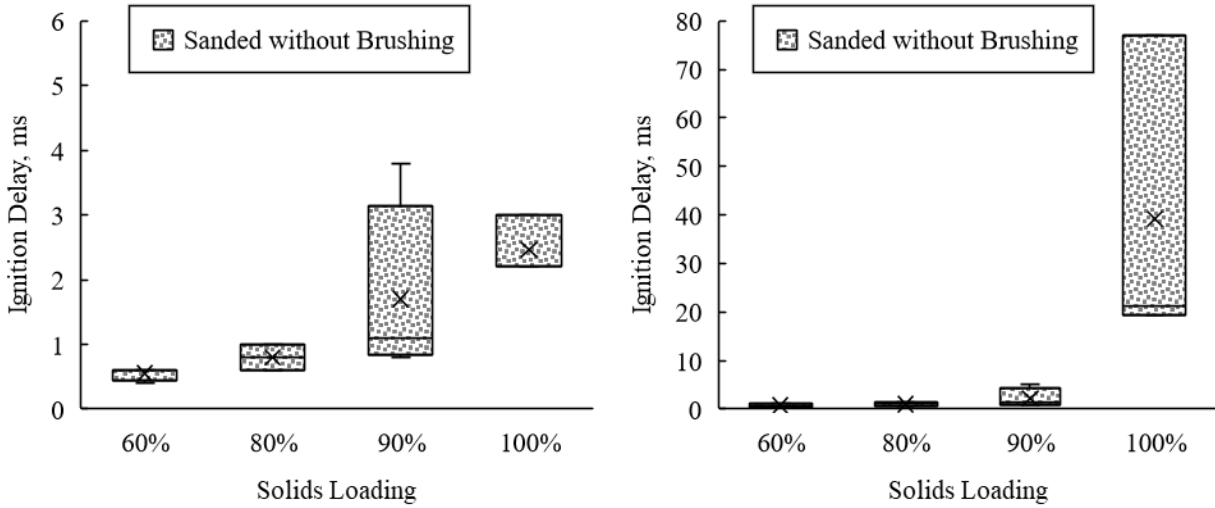


Figure 4.3. Ignition delay of AB pellets from which residual powder from sanding was not removed based on initial ignition (left) and main ignition (right).

Table 4.3. Numerical results of varying solids loading of sanded but unbrushed pellets.

Solids Loading	Initial ID, ms	Standard Deviation, ms	Main ID, ms	Standard Deviation, ms	# Tests
60%	0.55	0.09	0.70	0.30	4
80%	0.80	0.16	1.07	0.34	3
90%	1.70	1.22	2.20	1.66	4
100%	2.47	0.38	39.20	26.74	3

#### 4.2.2 Comparison to EDBB

Ignition delays for AB at various solids loadings and surface conditions were compared with EDBB results from Pfeil [1]. This comparison is shown in Table 4.4 and plotted in Figure 4.4. Note that brushing was not part of Pfeil’s sanding procedure, so his data for “sanded” pellets is listed here in the “Sanded without Brushing” category. It should also be noted that Pfeil pressed his pellets at a higher pressure and for a longer period of time. However, the AB pellets in this study were already measured to be in the mid to upper nineties for % TMD (percent of theoretical maximum density), so it is assumed that pressing these pellets at higher pressure or for a longer

duration would not have affected pellet density. Therefore, this difference in procedure was neglected and assumed to have no effect on ID.

In most cases, AB exhibited shorter IDs than the analogous EDBB pellets. It should be noted that while the surfaces of the unsanded AB pellets were pressed and therefore had more epoxy on the surface that had oozed out from between the AB particles, the surfaces of the unsanded EDBB pellets (except for the 100% pellets) were cut and therefore would have had more exposed fuel on the surface than the AB pellets. This makes AB's shorter IDs all the more notable. Exceptions to AB having a shorter ID are at 100% solids loading. However, Pfeil considered the times at 100% solids loading to be "violent reaction delays" (as opposed to ignition delays) in which the WFNA-EDBB reaction caused the WFNA to be rapidly expelled from the pellet, thus quenching the reaction [1, 2]. Pfeil and Dailey also showed AB having consistently shorter IDs compared to EDBB in pellet form with various binders and solids loadings, as well as in loose powder form [3].

Table 4.4. Comparison of AB initial ignition delays versus those of EDBB.

Solids Loading	Surface	AB			EDBB <sup>†</sup> [1]		
		ID, ms	Standard Deviation, ms	# Tests	ID, ms	Standard Deviation, ms	# Tests
30%	Unsanded	6.40*	0.45	4	-	-	-
30%	Sanded without Brushing	-	-	-	88	36.6	3
60%	Unsanded	8.23	1.39	6	9.2 <sup>‡</sup>	1.6	3
60%	Sanded without Brushing	0.55	0.09	4	3.3	0.5	3
80%	Unsanded	6.93	1.31	14	155 <sup>‡</sup>	29.7	2
80%	Sanded without Brushing	0.80	0.16	3	9.4	3	4
90%	Unsanded	10.55	1.09	4	-	-	-
90%	Sanded without Brushing	1.70	1.22	4	-	-	-
100%	Unsanded	-	-	-	2.9 <sup>§</sup>	0.3	6
100%	Sanded without Brushing	2.47	0.38	3	0 <sup>§</sup>	-	3

<sup>†</sup> Pfeil did not dry his EDBB powder before pressing into pellets [1].

<sup>‡</sup> The surfaces of Pfeil's unsanded EDBB pellets (except for 100% solids loading) were cut instead of pressed [1].

<sup>§</sup> Pfeil described the delays of 100% EDBB pellets as "violent reaction delays" instead of ignition delays [1].

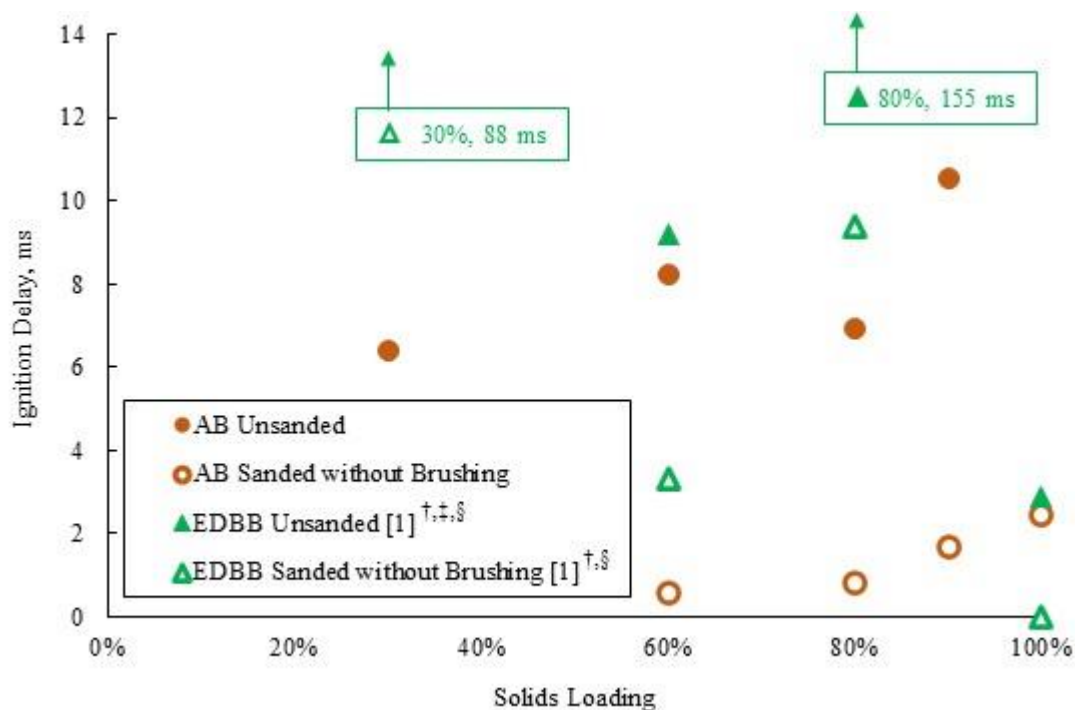


Figure 4.4. Graphical comparison of AB initial ignition delays versus those of EDBB.

### 4.2.3 Role of Binder

Plain epoxy pellets were tested to examine if the epoxy contributes to the reaction itself or if it simply protects the AB from moisture or assists with WFNA absorption or adhesion. While the epoxy pellets did not ignite, they did turn from clear into a rust color after coming into contact with WFNA, indicating some oxidation. The pellets retained this color in the interior even after the outsides of the pellets were rinsed with water as shown in Figure 4.5.



Figure 4.5. Untouched epoxy pellet (left) compared to epoxy pellet after being contacted with WFNA and rinsed with DI water (right).

Importantly, there was also much less splashing observed on the epoxy pellets than on the neat AB pellets. These observations indicate absorption or surface adhesion of the WFNA upon impact with the solid epoxy and suggest that while the epoxy does not directly contribute to the reaction, it does help facilitate it by reducing the amount of oxidizer splashed from the surface and holding it close to the fuel. A comparison of the period just after droplet impact for plain epoxy and neat AB pellets is shown in Figure 4.6. The syringe height was held constant at 127 mm (5 in) for both pellets.

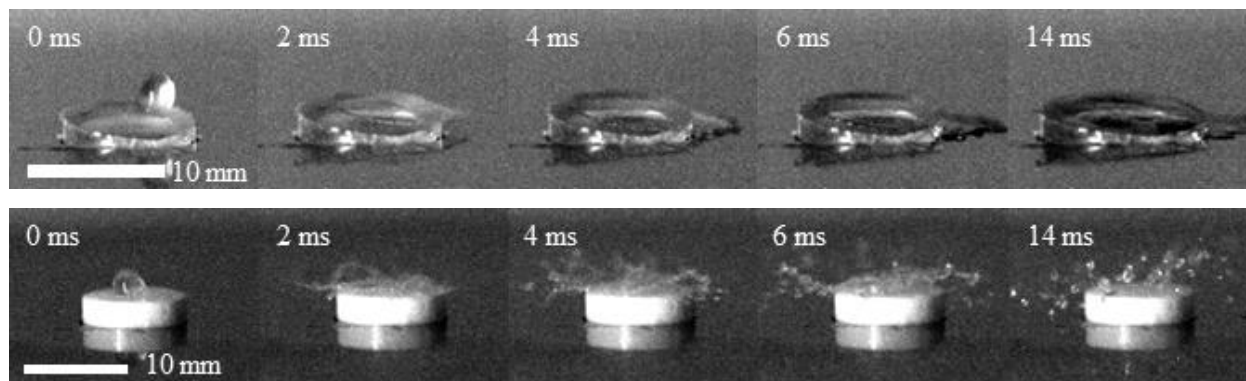


Figure 4.6. Comparison of WFNA splashing immediately following droplet impact with plain epoxy pellet (top) and neat AB pellet (bottom).

To further examine the interaction between WFNA and binder, wetting contact angle measurements were made between WFNA and neat samples of various binders that Pfeil used for ignition delay tests with EDBB [1]. The goal was to see if contact angle affects ignition delay. Pfeil generally found epoxy and RTV to have the shortest ignition delays and paraffin and HTPB to have the longest [1]. According to the results of the contact angle tests (presented in Table 4.5), paraffin has the highest contact angle (least wetting), and epoxy has one of the lowest (more wetting), which supports the hypothesis that lower contact angles (more wetting) leads to lower IDs. However, the RTV and HTPB contact angle results go against this hypothesis, at least as far as initial contact angle. Their steady state contact angles come out very similar, but it is assumed that only initial contact angle would matter on the short time scale of hypergolic ignition.

Table 4.5. Contact angles between WFNA and various binders.

Binder	Initial		Steady-State		# Tests
	Contact Angle, degrees	Standard Deviation, degrees	Contact Angle, degrees	Standard Deviation, degrees	
Epoxy	29.7	5.9	21.0	5.1	5
RTV	60.2	16.5	19.2	6.6	7
HTPB	32.7	3.8	20.8	4.1	3
R-45	35.2	6.0	-**	-	5
Paraffin <sup>††</sup>	60.9	4.4	60.9	4.4	4

To more clearly determine if there is a correlation between contact angle and ID, Pfeil's EDBB results were plotted in Figures 4.7-4.9 against the contact angle results presented. Each point of a given series is a different binder. The contact angle data is constant across the different plots. (None of the binder samples were sanded, and they all had 0% solids loading.) No correlation was apparent from this data.

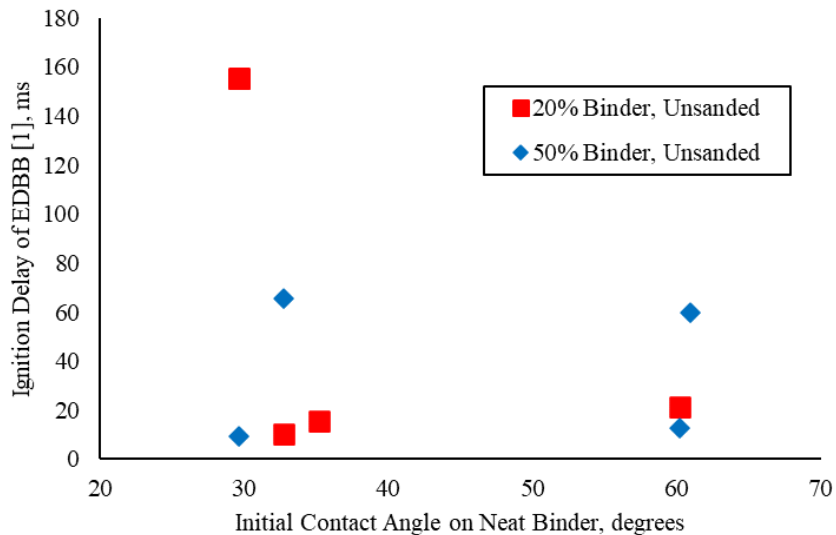


Figure 4.7. EDBB cut pellet ignition delays versus initial contact angles for the binders used.<sup>††§§</sup>

\*\* Steady-state contact angles could not be measured for R-45, because the R-45 appeared to react with the WFNA, obstructing the view of the droplet.

†† There was no distinguishable or measurable difference between initial and steady-state contact angles for paraffin, so these results were lumped together.

‡‡ HTPB data points in 50% binder series are actually 42% HTPB due to data available.

§§ R-45 data points in 20% binder series are actually 18% R-45 due to data available.

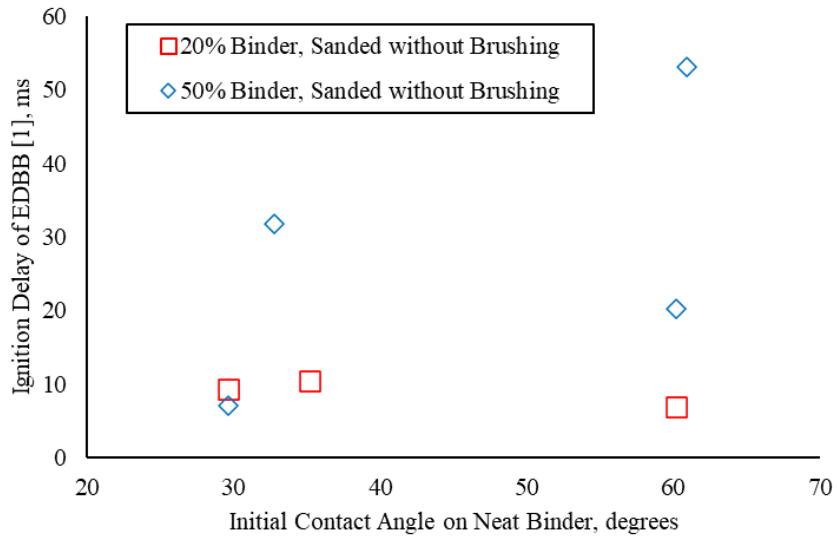


Figure 4.8. EDBB sanded pellet ignition delays versus initial contact angles for the binders used.<sup>††,§§</sup>

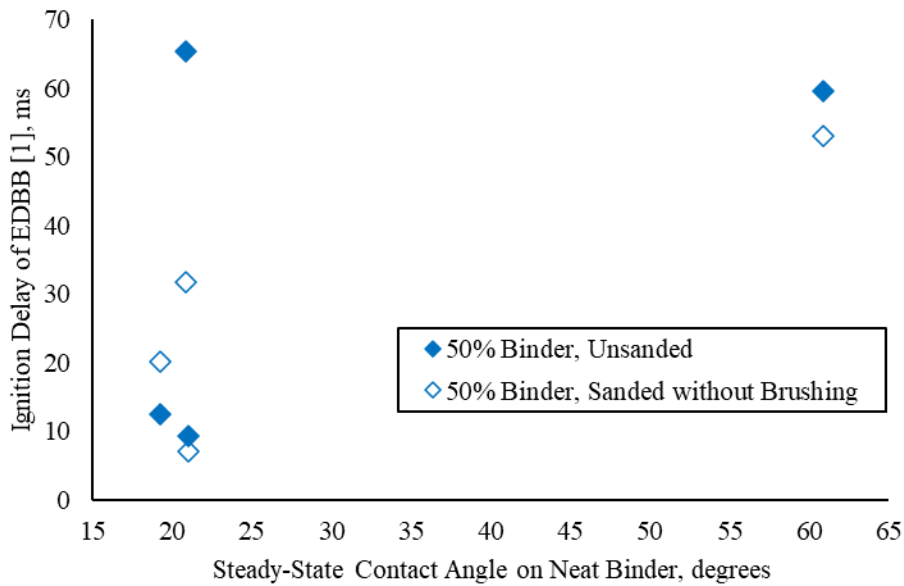


Figure 4.9. EDBB pellet ignition delays versus steady-state contact angles for the binders used.<sup>††</sup>

Aside from absorption or adhesion, the epoxy also slows the reaction between the WFNA and the AB. Although it is counterintuitive that a slower reaction would help ignition, this was demonstrated by Baier et al. [19]. Their attempts to hypergolically ignite a neat AB pellet with WFNA were unsuccessful, but they found hypergolic ignition with lower concentration (70%)

nitric acid to be reliable. They argued that the heat release from the reaction between neat AB and WFNA was so rapid that it resulted in film boiling. The resulting vapor layer prevented further reaction and ejected the WFNA from the surface. Pfeil and Pfeil et al. observed the same phenomenon between EDBB and WFNA and referred to the gas and WFNA expulsion as a “violent reaction” [1, 2].

#### **4.2.4 Reignition**

Lastly, AB pellets of different solids loadings were tested for their ability to reignite after being extinguished, because restart capability is very useful for rocket and spacecraft applications. Pellets were extinguished using compressed air as soon as possible after ignition. Once the camera was reset, another drop of WFNA was deposited on the pellet. The char layer on top of the previously ignited pellets resulted in longer IDs than those for the first WFNA drop. However, the ID itself was not of primary interest since it is heavily dependent on char layer thickness which depends on how long the pellet takes to extinguish and is difficult to control. In a motor, this would be heavily dependent on motor details. The main objective of reignition attempts was just to show that reignition is possible. Attempts were made to reignite AB pellets at solids loadings of 60%, 80%, 90% and 100%, for 2, 6, 2, and 2 pellets, respectively. All but one attempted relights were successful. The only unsuccessful attempt was an 80% AB pellet that took too long to extinguish and consequently developed a thick char layer. The extinguishing process was improved for the remaining samples. Therefore, this case was not included in the relight statistics, but the observation was noted. It is believed that such a char buildup would be less likely in a motor at sufficiently high pressure.

### **4.3 Storage Conditions**

To examine the effect of humidity on the AB pellets, some pellets were stored for one week in a separate container kept at 70%-80% RH after finishing curing in the dry box. This humidity was maintained using a water and sodium chloride (NaCl) mixture. Some pellets were sanded (and brushed) before being stored (pre-sanded), some were sanded (and brushed) immediately before testing, and some were left completely unsanded.

The results of this experiment are given in Figure 4.10 and Table 4.6. As expected, storing the pellets at a higher humidity resulted in longer IDs in the case of unsanded pellets. However, the large variation in ID among sanded pellets makes it unclear if the trend carries to the sanded case. The fact that the pre-sanded pellets had longer main IDs than those that were unsanded or not sanded until after leaving the humid environment supports the hypothesis that the epoxy may somewhat protect the AB from moisture. Even the longer IDs produced by the pre-sanded, humidly-stored pellets, however, were still shorter than many of the amines and amine-boranes examined by Pfeil [1] and Ramachandran et al. [5] and may still be short enough for use in a hybrid system. This demonstrates AB's storability in non-ideal environments. On a related note, it should be pointed out that the AB powder used in this study was synthesized almost 2 years prior to use, demonstrating AB's long-term storability. Before being dried and pressed into pellets, the AB spent most of its life in a sealed jar at ambient conditions.

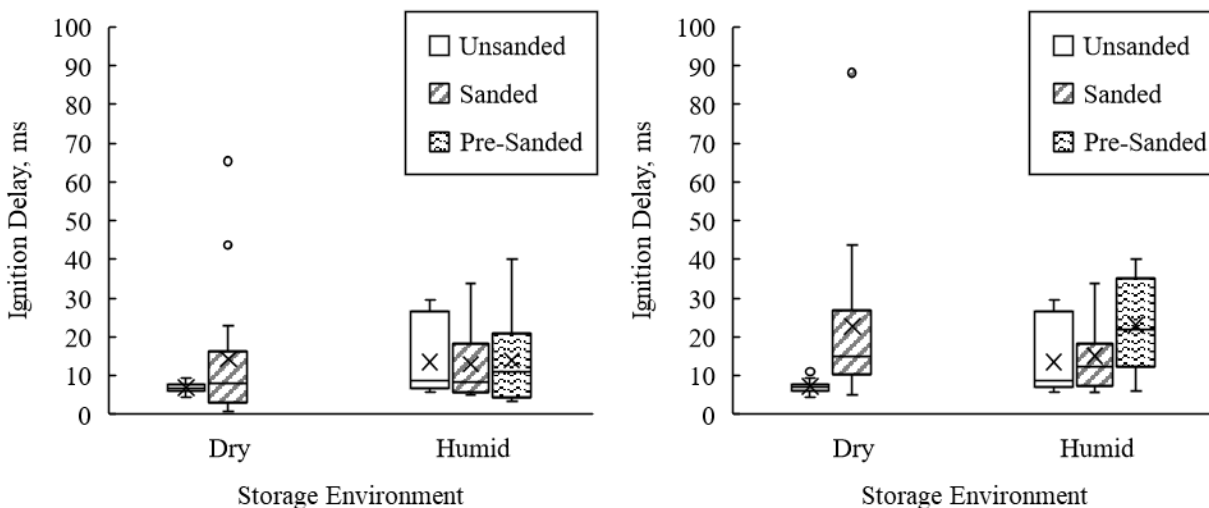


Figure 4.10. Ignition delay of 80% solids loading AB pellets as a function of pellet storage for initial ignition (left) and main ignition (right).

Table 4.6. Numerical results of varying storage humidity.

Storage Environment	Surface	Initial ID, ms	Standard Deviation, ms	Main ID, ms	Standard Deviation, ms	# Tests
Dry	Unsanded	6.93	1.31	7.16	1.59	14
Dry	Sanded	14.40	17.78	22.73	21.03	14
Humid	Unsanded	13.43	9.33	13.51	9.27	7
Humid	Sanded	13.00	9.47	15.11	8.80	7
Humid	Pre-sanded	14.07	12.36	23.03	12.05	6

In addition, humidly stored pellets were tested for their ability to reignite by the process discussed in Section 4.2.4. Of the six 80% AB pellets mentioned previously that were relit, 2 of them were stored dry, and 4 of them were stored in the humid environment. Two of the pellets stored at humidity were pre-sanded. The success of each of these relight attempts, especially those of the pre-sanded pellets, demonstrated that humidity does not prevent reignition.

Samples of loose AB powder were also stored in the humid environment for one week to be compared with control samples of powder stored in the dry box, and they were tested for purity. Purity was calculated based on hydrogen released after the AB was exposed to HCl as discussed previously in Section 3.1. Powder stored at humidity had a calculated purity of 89.6%. This is a negligible difference from the 89.5% purity measured for the powder stored in the dry box.

## 5. DISCUSSION AND CONCLUSION

Ignition delay of AB with WFNA was measured under a variety of configurations and experimental conditions. It was found that increasing the droplet impact velocity shortens ignition delay, at least for unsanded pellets. Pellets containing 80% AB produced the shortest average initial IDs of the pressed pellets without excess powder on top at 6.93 ms and 14.40 ms for unsanded and sanded pellets, respectively. The fact that the 80% AB pellets ignited more reliably than the 100% AB pellets suggests that the epoxy binder somehow facilitates the ignition process even if indirectly. The role of the epoxy was studied further, and it was found that the epoxy helps facilitate ignition by slowing the AB-WFNA reaction enough to prevent WFNA expulsion and by absorbing or adhering the WFNA droplet, thus holding it close to the AB fuel. Very short IDs resulting from pellets containing only 30% AB demonstrated that only a small amount of AB fuel is required to produce hypergolic ignition.

Across all experiments, sanding the pellets increased ID variation. Some pellets were sanded but were allowed to retain the resulting loose powder on their surfaces to show that IDs are expected to be shorter in an actual motor grain than in the experiments presented. 60% AB pellets exhibited the shortest average IDs of the solids loadings examined with this sanded but unbrushed surface condition. Average initial IDs of sanded but unbrushed pellets were less than 2.5 ms across all solids loadings and under 1 ms except for 90% and 100% AB. With the exception of the 100% AB pellets, even the average main IDs of pellets with this surface condition were extremely short at 0.70 ms, 1.07 ms, and 2.20 ms for 60%, 80%, and 90% solids loadings, respectively. This is important, because although initial ignition (defined by first visible light) is more commonly discussed in literature as a way to compare hypergolicity of different propellants, main ignition is the event more relevant to actual motor operation. Furthermore, even the longer IDs observed without the excess powder may still be sufficient for use in a hypergolic hybrid system due to the lowered risk of hard starts.

In an aging study in which some pellets were stored for a week at 70-80% RH as opposed to 10-13% RH, it was observed that the pellets sanded before exposure to the higher humidity had longer IDs than those sanded after. This result suggests that the epoxy may also partially protect the AB from moisture. At least in the unsanded cases, the pellets stored in a humid environment

also had longer IDs than those stored in a dry environment. It should be noted, however, that even the longer IDs observed due to humidity may still be acceptable in some applications.

Lastly, pellets of varying solids loadings and storage humidities were extinguished after their initial ignition and contacted with WFNA again. Reignition attempts of all pellet types tested were successful, demonstrating that it is feasible to restart an AB motor.

In addition to confirming AB's short IDs, this work has demonstrated the importance of fuel grain surface conditions, investigated the effect of oxidizer droplet impact velocity, examined the role of binder in an AB system, studied the effect of humidity on AB, and proven reignition capability. This knowledge is critical if AB is to be used in real motor applications.

# APPENDIX A. WFNA TRANSFER PROCEDURE



**Procedure For:** Transfer of WFNA from 500 mL container to 7.5 mL vials

---

**Date Created/Created By:** 11/13/18 Kate Clements

---

**Location:** ZL4 115, ZL6

---

**Notes:**

**Potential hazards and Mitigation:**

- WFNA spill – Use of PPE (chemical resistant gloves, sleeves, eye protection, face shield, Tyvek suit, chemical resistant boots), DI water and NaOH on hand to dilute/neutralize if necessary.
- Inhalation of WFNA fumes – Use of fume hood and NO<sub>2</sub> sensor.
- Unforeseen circumstances/accidents – Two people present throughout procedure.

**Section 1 – PPE to be used during handling of WFNA**

- 1. Tyvek suit
- 2. Chemical resistant gloves (go over nitrile gloves)
- 3. Chemical resistant boots
- 4. Poly sleeves
- 5. Safety glasses
- 6. Face Shield
- 7. Hearing protection
- 8. Long pants
- 9. Close-toed shoes

**Section 2 – Materials/equipment required**

- 1. Glove bag
- 2. Fume hood
- 3. NO<sub>2</sub> sensor
- 4. O<sub>2</sub> sensor
- 5. Argon gas cylinder

- a. Note: Nitrogen would also be acceptable, but argon cylinder already in place (with tubing) in ZL6.
- 6. PTFE vial holder
- 7. 7.5 mL vials (6) with caps, can fill more if desired
- 8. Ziploc gallon freezer bag (1)
- 9. Ziploc quart freezer bag (1)
- 10. Smaller Ziploc bags (6, or as many bags as vials to be filled)
- 11. Painter's tape/duct tape
- 12. Scissors
- 13. 5 mL syringe
- 14. PTFE sheet
- 15. Mini fridge
- 16. Weight
- 17. Magnet
- 18. DI water (squeeze bottle and jug)
- 19. Kimwipes
- 20. Small beaker (for small amount of DI water for cleaning syringe)
- 21. Medium beaker (for WFNA)
- 22. Large beaker (for holding used Kimwipes and excess WFNA until neutralization)
- 23. pH strips
- 24. Tweezers
- 25. NaOH pellets
- 26. NaOH-water solution
- 27. Spatula/stir rod

### Section 3 – Preparation for Transfer

- 1. NOTE: This procedure (Sections 3-5) requires two people at all times.
- 2. Test each vial/cap combination to make sure each cap screws on and off its vial easily. If there are any issues with this (e.g. threads not lining up well), discard and replace with different vial/cap.
- 3. Both parties, don general PPE (safety glasses and nitrile gloves).
- 4. Clear out ZL6 fume hood, and wipe down surface.
- 5. Set glove bag in fume hood. Use magnet(s) to secure the back of the glove bag to back of fume hood at some height so that front of bag will fit inside fume hood after sealing while leaving enough bag height to work in.
- 6. Place PTFE sheet inside glove bag as a protective working surface.
- 7. Place vial holder, vials (with caps), O<sub>2</sub> sensor (turned on), medium beaker, large beaker, Kimwipe box, and syringe in glove bag. Vials should be inside vial holder with their caps separately on the side.

- 8. Connect regulator and tubing to argon cylinder in ZL6 if disconnected.
- 9. Cut small hole in one of glove bag ports on the right (closest to argon tube).
- 10. Place argon tube through the hole to the main section of the bag (so that incoming gas does not directly impinge the bag as this could create a puncture).
- 11. Tape the connection between the bag port and the tube so that it is sealed.
- 12. Cut small hole in back port on left side of bag (closest to unoccupied side of fume hood) to serve as a vent.
- 13. Both parties, don WFNA-specific PPE (chemical resistant gloves and boots, sleeves, Tyvek suit, face shield).
- 14. Turn on NO<sub>2</sub> sensor.

#### **Section 4 – WFNA Transfer**

- 1. Crack open door to mini fridge in 115 of ZL4 and hold NO<sub>2</sub> sensor near opening to check for fumes.
- 2. If there is no indication of fumes, carefully remove WFNA container from fridge, bring to ZL6, and place in glove bag. The WFNA container shall be carried with two hands.
  - a. The second person shall be responsible for opening doors and keeping the sensor close to the WFNA container. Once the WFNA container is in the glove bag, he/she shall affix the NO<sub>2</sub> sensor to the primary's suit or place it on the sill of the fume hood.
- 3. Double-check that all required supplies are inside glove bag.
- 4. Second person, roll up front of glove bag, and seal with strip provided and additional tape if needed. After this is completed, second person may now remove WFNA-specific PPE and remain in safety glasses and nitrile gloves if desired.
- 5. Secondary, begin argon flow, setting regulator to 5-10 psi. (It can be run higher for a little bit, but keep an eye on the bag, as it will inflate quickly.) Let run at least until the O<sub>2</sub> sensor reads <1.5 ppm. (In its currently uncalibrated state, the minimum reading is -0.7 ppm.)
- 6. Don hearing protection if argon flow is loud or if O<sub>2</sub> meter is not muted. Both parties will need it, but second person should put it on for primary, as primary's gloves may be contaminated with WFNA from carrying container.
- 7. Place weight over vent port to stop venting, and turn argon flow down to a trickle. The weight and argon flow can be adjusted further so that there is no net inflation or deflation.
- 8. Primary, place hands in gloves of glove bag. (Chemical resistant gloves shall remain on, even while using the glove box gloves.)
- 9. Open large WFNA container.

- 10. Very carefully, pour 40 mL (or slightly more for margin) WFNA from large container into medium beaker.
- 11. Close large WFNA container.
- 12. Fill syringe from large beaker, and empty into first vial.
  - a. Repeat until each vial has had one syringe-full (5 mL).
  - b. If there are any drips or spills, wipe them up with a Kimwipe, and put Kimwipe in large beaker.
- 13. Fill syringe, and put roughly 1.6 mL (one-third of syringe) into each of the first through third vials.
  - a. Repeat with fourth through sixth vials.
- 14. Carefully set down syringe.
- 15. Screw caps onto vials with the vials remaining in the holders.
- 16. Very carefully, pull the first vial out of the vial holder by its cap and tighten cap, being careful to keep vial vertical the whole time. Return to vial holder.
  - a. Repeat for each vial.
- 17. Remove weight to open vent port, and increase argon flow. Let run for 10 minutes to purge any WFNA fumes.
- 18. Turn off argon flow, and disconnect from glove bag.
- 19. Secondary, put WFNA-specific PPE back on.
- 20. Secondary, unseal front of glove bag. Primary, remove all glove bag contents. They shall be placed in the unoccupied part of the fume hood.
- 21. Primary, place the large WFNA container back in its Ziploc gallon freezer bag.
- 22. Double-check that the caps are securely tightened on the vials. Place the vials in individual smaller Ziploc bags, and then place those bags inside of a Ziploc quart freezer bag.

### Section 5 – Storage and Clean-up

- 1. Carefully bring bags with WFNA to ZL4 and place inside mini fridge in 115.
  - a. The second person shall be responsible for opening doors and keeping the sensor close to the WFNA containers.
- 2. NOTE: Second person may remove his/her WFNA-specific PPE (chemical resistant gloves and boots, sleeves, Tyvek suit, face shield) once the WFNA is stored in fridge so that they may better assist putting cleaned equipment away, turning sink on/off, etc. However, primary must remain in full PPE while cleaning anything that could have been in contact with WFNA, including glove bag.
- 3. Primary, wipe down sheet, vial holder, outside of syringe, and anything else that could have been contacted by WFNA or contaminated gloves with DI water and Kimwipes. Put used Kimwipes in large beaker, and fill partially with water.
- 4. Secondary, fill small beaker with DI water. Primary, fill syringe from this beaker and empty syringe into large beaker to clean inside of syringe. Repeat at least 3 times.

- 5. Primary, mix contents of large beaker, and test pH using pH strips. pH strips should be given to you by secondary. Primary should use tweezers to grab them.
  - a. If pH < 6, add NaOH pellets (given in separate container from secondary to primary), stir, and re-test. Repeat until sufficiently neutralized.
  - b. If you overshoot and pH > 8, repeat step 5.a using citric acid powder instead of NaOH pellets.
- 6. Primary, thoroughly rinse out used Kimwipes in ZL6 sink. Then place in a Ziploc freezer bag, and throw away.
- 7. Wash beakers in ZL6 sink with soap and water.
- 8. Assess glove bag condition, and decide what to do with it.
  - a. If there were no spills (touching the glove bag) or punctures and the bag will be reused, use DI water and Kimwipes to clean off glove bag gloves, fold glove bag and store for future use. Be sure to mark that it was used with WFNA and to wear PPE and sensor when handling bag.
  - b. If there were spills, carefully REM glove bag.
  - c. If there are punctures, dispose of bag.
- 9. Wipe down surface of fume hood with DI water.
- 10. Primary, wash gloves with soap and water before removing and storing. Remove WFNA-specific PPE. Still wear safety glasses and nitrile gloves.
- 11. Wipe down everything with DI water one more time. (The Kimwipes used on this final cleaning can be thrown in the trash.)
- 12. Store beakers, syringe, vial holder, and PTFE sheet.

#### **Section 6 – Emergency Procedures**

- 1. WFNA spill: Minor spill may be wiped up with Kimwipes and water (while wearing full PPE). NaOH-water solution may be used towards neutralization if desired, but exercise caution, and remember that a dilute solution will not neutralize very much. In the event of a major spill, secure the area/leave if necessary and contact a supervisor.
- 2. Unintentional ignition of material resulting in bodily injury: If minor injury is sustained from the incident (e.g., minor burns), treat with appropriate first aid and contact a supervisor. If major injury is sustained, immediately call 911 and then contact a supervisor.
- 3. Unintentional ignition of material resulting in uncontrolled fire: Ensure that fire is extinguished using appropriate fire extinguisher and then contact a supervisor. If fire is sufficiently uncontrolled, immediately pull a fire alarm, evacuate the building, call 911, and then contact a supervisor. If a fire is sufficiently controlled, let the fire self-extinguish, and then contact a supervisor.
- 4. Detected NO<sub>2</sub> leak: Close fume hood sash, leave room, and contact a supervisor.



- 5. Unforeseen injury: If minor injury is sustained from the incident (e.g., cuts, minor burns, etc.), treat with appropriate first aid and immediately contact a supervisor. If major injury is sustained, call 911 and then contact a supervisor.

**Contact Information**

Jason Gabl: 847-309-4555

Dr. Son: 765-337-8204

Tim Manship: 775-225-1464

Dr. Pourpoint: 765-494-9423

<b>Approved By:</b>	Steven Son _____ <small>Steven Son</small>	11/14/18 _____ <small>Date</small>
<b>Approved Members:</b>	Kate Clements _____ _____	11/14/18 _____ _____

# APPENDIX B. DROPLET TEST PROCEDURE



**Procedure For:** Ignition Delay Tests using WFNA Droplets

---

**Date Created/Created By:** 11/28/18 Kate Clements

---

**Location:** ZL4 115B, ZL6

---

**Notes:**

**Potential hazards and Mitigation:**

- WFNA spill – Use of PPE (chemical resistant gloves, sleeves, eye protection, face shield, Tyvek suit, chemical resistant boots), DI water and NaOH on hand to dilute/neutralize if necessary.
- Inhalation of WFNA fumes – Use of fume hood and NO<sub>2</sub> sensor.
- Unforeseen circumstances/accidents – Two people present throughout procedure.

**Section 1 – PPE to be used during handling of WFNA**

- 1. Tyvek suit
- 2. Chemical resistant gloves (go over nitrile gloves)
- 3. Chemical resistant boots
- 4. Poly sleeves
- 5. Safety glasses
- 6. Face Shield
- 7. Long pants
- 8. Close-toed shoes

**Section 2 – Materials/equipment required**

- 1. Fume hood
- 2. NO<sub>2</sub> sensor
- 3. PTFE single vial holder w/ set screw
- 4. Ziploc gallon freezer bags (2)
- 5. Small plastic bag (1)
- 6. 100 µL syringe
- 7. Syringe holder test apparatus

- 8. Allen wrenches
- 9. Wrench
- 10. Shop lamp
- 11. 100 grit sandpaper
- 12. Small paint brush
- 13. Ruler
- 14. PTFE sheet
- 15. Mini fridge
- 16. DI water (squeeze bottle and jug)
- 17. Kimwipes
- 18. Small beaker
- 19. Large beakers (2)
- 20. pH strips
- 21. Tweezers
- 22. NaOH pellets
- 23. 5 wt% NaOH solution (squeeze bottle)
- 24. Spatula/stir rod
- 25. Disposable transfer pipette
- 26. Painter's tape
- 27. Weigh boat
- 28. Camera(s)
- 29. Tripod(s)
- 30. Laptop(s)

### Section 3 – Preparation

- 1. Clear out 115 fume hood, and wipe down surface.
- 2. Assemble test apparatus, and place on PTFE sheet in fume hood.
- 3. Fill small beaker with DI water.
- 4. Set up camera on tripod. (If multiple cameras are being used, mount on optics board instead. If using an optics board, it should be put on a cart to achieve the proper height.) The focus should be the circle cutout where the pellet goes. This should be towards the bottom of the frame.
- 5. Set shop lamp on tall chair facing fume hood, and shield with aluminum foil. Test lamp shielding to make sure that sample location is illuminated without shining in primary's eyes.
- 6. Fill one large beaker about half full with water. (Tap water is fine.) Place this beaker and the other large beaker in the fume hood.

#### Section 4 – Experiment

- 1. Remove desired pellets from dry box, and reseal dry box with painter’s tape.
- 2. If desired to find %TMD (% of theoretical maximum density) of pellets, measure diameter, thickness, and mass of a few pellets.
- 3. NOTE: The remaining parts of the procedure (Sections 4-5) require two people at all times. All steps will be performed by the primary unless otherwise stated.
- 4. Both parties, don WFNA-specific PPE (chemical resistant gloves and boots, sleeves, Tyvek suit, face shield) on top of normal PPE (safety glasses and nitrile gloves).
- 5. Turn on NO<sub>2</sub> sensor.
- 6. Crack open door to mini fridge in 115B, and hold NO<sub>2</sub> sensor near opening to check for fumes.
- 7. If there is no indication of fumes, carefully remove bag of WFNA vials. Carry with two hands to fume hood.
  - a. The secondary shall be responsible for opening the fridge door and keeping the sensor close to the WFNA container. Once the WFNA container is in the fume hood, he/she shall affix the NO<sub>2</sub> sensor to the primary’s suit or place it on the sill of the fume hood.
- 8. Carefully remove one small bag containing one WFNA vial, keeping both the small bag and the larger bag of vials in the fume hood at all times. Close and return large bag of vials to fridge, carrying with two hands. Fridge door shall be opened and closed by secondary.
- 9. Secondary, remove WFNA-specific PPE (chemical resistant gloves and boots, sleeves, Tyvek suit, face shield). All further operations inside fume hood or with items that could have been in contact with WFNA or the primary will be handled solely by the primary.
  - a. NOTE: If at any point the primary drops a tool that is needed to continue, the secondary shall pick it up with a clean tool and place it on the fume hood sill.
- 10. Open small vial bag, and remove vial. Place in PTFE vial holder, and secure using set screw.
  - a. NOTE: Be careful not to overtighten the set screw as this will cause the vial to break. The set screw should only be as tight as it needs to be to hold the body of the vial in place when the cap is twisted open or closed.
- 11. Keeping vial vertical and inside fume hood, remove cap, and fill syringe. Carefully set syringe down on small plastic bag and put cap back on vial.
- 12. Place syringe in holder on test apparatus, and use ruler to adjust syringe tip to desired height. Test drop placement, adjusting plate and PTFE arm position as needed until the drop lands perfectly inside the circle cut-out of the plate. Verify that the syringe tip is still at the desired height after alignment.

- a. Any drops of WFNA shall be wiped up using DI water (from squeeze bottle) and Kimwipes. These Kimwipes shall be placed in large beaker with water after use.
- 13. Secondary, remove a pellet from container, and place on sill of fume hood, being careful not to have hand inside fume hood or to touch anything primary has touched.
  - a. If sanding is desired, the secondary shall sand the pellet before placing on fume hood sill. Sanding shall be performed using 100 grit sandpaper and excess powder brushed off into weigh boat using a paint brush.
- 14. Primary, use tweezers to place pellet in circle cut-out on apparatus.
- 15. Secondary, confirm that camera is focused on pellet surface. The camera should be looking very slightly down on the pellet so that the whole depth of the top surface can be seen rather than just the front. However, the video should still be mostly from the front (horizontal) so that the time of pellet-droplet contact will be easy to distinguish later.
- 16. Secondary, set camera to desired frame rate, video dimensions, and exposure time if not done already. The exposure time should be the maximum allowable for the given frame rate. If you manually type in an exposure time, you should get a higher exposure time than is available from the dropdown menu. Cover camera lens and run a CSR.
- 17. Primary, verify with secondary that camera is set and ready to record. Release drop of WFNA onto pellet.
  - a. Secondary should trigger camera(s) at first light. (Camera should be set to record before and after trigger.) Note the pellet number, solids loading, surface condition (sanding), etc. as well as syringe height in notebook for each run, so that conditions may be looked up by video number. Also, be sure to note camera settings, as well as humidity and temperature in 115B on test day.
- 18. Extinguish flame with DI water. Wipe up liquid with Kimwipe, and put in large beaker with water (WFNA waste). Pick up charred pellet with Kimwipe and place in other large beaker (dry waste).
  - a. NOTE: Even if pellet does not ignite, spray water on it and wait a few seconds before picking it up or wiping up WFNA. Sometimes reactions are delayed, and the pellet eventually ignites when not expected.
- 19. Secondary, save video using test number as file name.
- 20. Repeat Steps 13-19 (minus the camera settings) for as many runs as desired. Refill syringe as needed according to Step 9. Primary may clean gloves when necessary using DI water and Kimwipes and placing used Kimwipes in WFNA waste beaker.

### **Section 5 – Clean-up**

- 1. Fill syringe from with DI water from small beaker and empty syringe into large beaker with water to clean inside of syringe. Repeat at least 3 times.
- 2. Use disposable pipette to carefully empty remaining WFNA in vial into large beaker with water. Rinse vial with DI water and dump this water into beaker. Clean disposable pipette with water as described for the syringe in Step 1. Put pipette and vial aside in fume hood to be REMed with other materials. Do not throw away.

- 3. Wipe down all surfaces and objects that may have come into contact with WFNA using DI water and Kimwipes. This will require partially disassembling the test apparatus so that the plates and inner portion of syringe holder may be accessed. Place all used Kimwipes in WFNA waste beaker.
- 4. Dump any remaining DI water in small beaker into WFNA waste beaker, and carefully stir contents.
- 5. Secondary, tear small pH strip and leave on fume hood sill. Primary pick this up with tweezers and place in WFNA waste beaker. If  $\text{pH} < 6$ , have secondary put NaOH pellets in container and hand it to primary who will stir into beaker, and re-test. Repeat until sufficiently neutralized.
  - a. If you overshoot the neutralization ( $\text{pH} > 8$ ), add citric acid powder to balance it. Again, secondary should put citric acid in a container to hand to primary.
- 6. Carefully bring beaker to ZL6 (holding with two hands). Thoroughly rinse out WFNA debris in ZL6 sink. Then place in a Ziploc freezer bag, and throw away. Wash beaker using soap and water. Wash small beaker as well.
  - a. Secondary shall open doors, turn sink on/off, hold Ziploc bag open, squirt soap, dry beaker, etc.
- 7. Place contents from other beaker (dry debris, charred fuel pellets, etc.) in Ziploc freezer bag and set aside to be REMed. Secondary should add used sandpaper and the weigh boat of excess powder to this bag as well. Wash beaker in ZL6 sink as described in Step 6.
- 8. While still wearing them, wash chemical resistant gloves in ZL6 sink with soap and water. Place on drying rack in 115B.
- 9. Primary, remove WFNA-specific PPE.
- 10. Wipe down everything with DI water and Kimwipes one more time, and then store.
- 11. REM vial, small vial bag, and disposable pipette. (They should be in a separate REM bag than the dry AB waste.)
- 12. Wipe down surface of fume hood with DI water.

### Section 6 – Emergency Procedures

- 1. Unintentional ignition of material resulting in bodily injury: If minor injury is sustained from the incident (e.g., minor burns), treat with appropriate first aid and contact a supervisor. If major injury is sustained, immediately call 911 and then contact a supervisor.
- 2. Unintentional ignition of material resulting in uncontrolled fire: Ensure that fire is extinguished using appropriate fire extinguisher and then contact a supervisor. If fire is sufficiently uncontrolled, immediately pull a fire alarm, evacuate the building, call 911, and then contact a supervisor. If a fire is sufficiently controlled, let the fire self-extinguish, and then contact a supervisor.



- 3. Detected NO<sub>2</sub> leak: Close fume hood sash, leave room, and contact a supervisor.
- 4. Unforeseen injury: If minor injury is sustained from the incident (e.g., cuts, minor burns, etc.), treat with appropriate first aid and immediately contact a supervisor. If major injury is sustained, call 911 and then contact a supervisor.

**Contact Information**

Jason Gabl: 847-309-4555

Dr. Son: 765-337-8204

Tim Manship: 775-225-1464

Dr. Pourpoint: 765-494-9423

**Approved By:**

Steven Son

11/28/18

\_\_\_\_\_  
Steven Son

\_\_\_\_\_  
Date

**Approved Members:**

Kate Clements

Michael Baier

_____	_____
_____	_____
_____	_____
_____	_____
_____	_____
_____	_____
_____	_____

## REFERENCES

- [1] Pfeil, M. A., “Solid Amine-Boranes as High Performance Hypergolic Hybrid Rocket Fuels and Their Combustion Behavior in a Hypergolic Hybrid Combustor,” Ph.D. Dissertation, Aeronautics and Astronautics Dept., Purdue Univ., West Lafayette, IN, 2014.
- [2] Pfeil, M. A., Dennis, J. D., Son, S. F., Heister, S. D., Pourpoint, T. L., Ramachandran, P. V., “Characterization of Ethylenediamine Bisborane as a Hypergolic Hybrid Rocket Fuel Additive,” *Journal of Propulsion and Power*, Vol. 31, No. 1, 2015, pp. 365-372.  
doi: 10.2514/1.B35386
- [3] Pfeil, M. A. and Dailey, J. M., “Hypergolic Hybrid Fuel Grain Compatibility Studies Using Various Binders in Conjunction with Ammonia Borane and Ethylenediamine-Bisborane,” *Joint Army-Navy-NASA-Air Force (JANNAF) Meeting*, Paper 2016-0006FL, Phoenix, AZ, Dec. 2016.
- [4] Pfeil, M. A., Kulkarni, A. S., Ramachandran, P. V., Son, S. F., Heister, S. D., “Solid Amine-Boranes as High-Performance and Hypergolic Hybrid Rocket Fuels,” *Journal of Propulsion and Power*, Vol. 32, No. 1, Jan.-Feb. 2016, pp. 23-31.  
doi: 10.2514/1.B35591
- [5] Ramachandran, P. V., Kulkarni, A. S., Pfeil, M. A., Dennis, J. D., Willits, J. D., Heister, S. D., Son, S. F., Pourpoint, T. L., “Amine-Boranes: Green Hypergolic Fuels with Consistently Low Ignition Delays,” *Chemistry: A European Journal*, Vol. 20, No. 51, 2014, pp. 16869-16872.  
doi: 10.1002/chem.201405224
- [6] Baier, M. J., Ramachandran, P. V., Son, S. F., “Characterization of the Hypergolic Ignition Delay of Ammonia Borane,” *Journal of Propulsion and Power*, Vol. 35, No. 1, Jan. 2019.  
doi: 10.2514/1.B37075
- [7] Weismiller, M. R., Connell Jr., T. L., Risha, G. A., Yetter, R. A., “Characterization of Ammonia Borane (NH<sub>3</sub>BH<sub>3</sub>) Enhancement to a Paraffin Fueled Hybrid Rocket System,” *46th AIAA/ASME/SAE/ASEE Joint Propulsion Conference & Exhibit*, AIAA Paper 2010-6639, Nashville, TN, 2010.  
doi: 10.2514/6.2010-6639
- [8] Benhidjeb-Carayon, A., Gabl, J., Pourpoint, T. L., “Hypergolicity of Mixed Oxides of Nitrogen with Solid Fuels for Hybrid Rocket Application,” *53rd AIAA/SAE/ASEE Joint Propulsion Conference, AIAA Propulsion and Energy Forum*, AIAA Paper 2017-4848, Atlanta, GA, 2017.  
doi: 10.2514/6.2017-4848

- [9] Jain, S. R. and Rajendran, G., "Chemical Aspects of the Hypergolic Preignition Reactions of Some Hybrid Hypergols," *Combustion and Flame*, Vol. 67, No. 3, March 1987, pp. 207-215.  
doi: 10.1016/0010-2180(87)90096-4
- [10] Jain, S. R., Rao, R., Murthy, K. N., "Studies on the Synergistic Hypergolic Ignition of Hybrid Systems," *Combustion and Flame*, Vol. 71, No. 3, March 1988, pp. 233-243.  
doi: 10.1016/0010-2180(88)90061-2
- [11] Bernard, M. L., Cointot, A., Auzanneau, M., Sztal, B., "The Role of Surface Reactions in Hypergolic Ignition of Liquid-Solid Systems," *Combustion and Flame*, Vol. 22, No. 1, Feb. 1974, pp. 1-7.  
doi: 10.1016/0010-2180(74)90002-9
- [12] Munjal, N. L. and Parvatiyar, M. G., "Ignition of Hybrid Rocket Fuels with Fuming Nitric Acid as Oxidant," *Journal of Spacecraft and Rockets*, Vol. 11, No. 6, 1974, pp. 428-430.  
doi: 10.2514/3.62093
- [13] Jain, S. R., Krishna, P. M. M., Verneker, V. R., "Effect of Variables on Ignition Delays of Hydrazone/Nitric Acid Systems," *Propellants, Explosives, Pyrotechnics*, Vol. 5, No. 5, Oct. 1980, pp. 135-138.  
doi: 10.1002/prop.19800050504
- [14] Jain, S. R., Murthy, K. N., Thanoo, B. C., "Ignition Delay Studies on Hypergolic Fuel Grains," *Defence Science Journal*, Vol. 38, No. 3, July 1988, pp 273-286.  
doi: 10.14429/dsj.38.5849
- [15] Kulkarni, S. G. and Panda, S. P., "Role of Thermal Degradation of Hybrid Rocket Fuels in Hypergolic Ignition and Burning with RFNA as Oxidizer," *Combustion and Flame*, Vol. 39, No. 2, Oct. 1980, pp. 123-132.  
doi: 10.1016/0010-2180(80)90012-7
- [16] Mullins, B. P., "Spontaneous Ignition of Liquid Fuels," *Butterworths Scientific Publications*, London, 1955.
- [17] Anderson, R., Brown, R. S., Thompson, G. T., Ebeling, R. W., "Theory of Hypergolic Ignition of Solid Propellants," *AIAA Heterogeneous Combustion Conference*, Palm Beach, FL, 1963.  
doi: 10.2514/6.1963-514
- [18] Spengler, G., Lepie, A. H., Bauer, J., "Measurements of Ignition Delays of Hypergolic Liquid Rocket Propellants," *Spring Meeting, Western States Section – The Combustion Institute*, ASME Paper WSS/CI 64-12, Stanford University, April 1964.

- [19] Baier, M. J., McDonald, A. J., Clements, K. A., Goldenstein, C. S., Son, S. F., “High-Speed Multi-spectral Imaging of the Hypergolic Ignition of Ammonia Borane,” *Proceedings of the Combustion Institute*, 2020. (submitted)
- [20] Cortopassi, A. C. and Boyer, J. E., “Hypergolic Ignition Testing of Solid Fuel Additives with MON-3 Oxidizer,” *53rd AIAA/SAE/ASEE Joint Propulsion Conference, AIAA Propulsion and Energy Forum*, AIAA Paper 2017-5050, Atlanta, GA, 2017.  
doi: 10.2514/6.2017-5050
- [21] Ramachandran, P. V. and Kulkarni, A. S., “Water-Promoted, Safe and Scalable Preparation of Ammonia Borane,” *International Journal of Hydrogen Energy*, Vol. 42, No. 2, 2017, pp. 1451–1455.  
doi: 10.1016/j.ijhydene.2016.06.231
- [22] Rassat, S. D., Aardahl, C. L., Autrey, T., Smith, R. S., “Thermal Stability of Ammonia Borane: A Case Study for Exothermic Hydrogen Storage Materials,” *Energy & Fuels*, Vol. 24, No. 4, 2010, pp. 2596-2606.  
doi: 10.1021/ef901430a
- [23] Bowden, M., Autrey, T., Brown, I., Ryan, M., “The Thermal Decomposition of Ammonia Borane: A Potential Hydrogen Storage Material,” *Current Applied Physics*, Vol. 8, No. 3-4, May 2008, pp. 498-500.  
doi: 10.1016/j.cap.2007.10.045
- [24] Zhang, J., Zhao, Y., Akins, D. L., Lee, J. W., “Thermal Decomposition and Spectroscopic Studies of Preheated Ammonia Borane,” *Journal of Physical Chemistry*, Vol. 114, No. 45, 2010, pp. 19529-19534.  
doi: 10.1021/jp105014t
- [25] Heister, S. D., Anderson, W. E., Pourpoint, T. L., Cassady, R. J., “Liquid Rocket Engines,” *Rocket Propulsion*, 1<sup>st</sup> ed., Cambridge University Press, New York, 2019, pp. 313-315.  
doi: 10.1017/9781108381376

## **PUBLICATIONS**

### **PUBLICATIONS**

(submitted) M. J. Baier, A. J. McDonald, K. A. Clements, C. S. Goldenstein, S. F. Son, “High-Speed Multi-spectral Imaging of the Hypergolic Ignition of Ammonia Borane,” *Proceedings of the Combustion Institute*, 2020.

(submitted) K. A. Clements, M. J. Baier, P. V. Ramachandran, and S. F. Son, “An Experimental Study of Factors Affecting Hypergolic Ignition of Ammonia Borane,” *Journal of Propulsion and Power*, 2020.

### **CONFERENCE PAPERS**

K. A. Clements, M. J. Baier, P. V. Ramachandran, and S. F. Son, “An Experimental Study of Factors Affecting Hypergolic Ignition of Ammonia Borane,” *AIAA Propulsion and Energy Forum*, Indianapolis, IN, 2019.